7-2006

Dissolution, Reactor, and Environmental Behavior of ZrO 2 -MgO Inert Fuel Matrix Neutronic Evaluation of MgO-ZrO2 Inert Fuels

E. Fridman
Ben-Gurion University of the Negev, emilf@bgu.ac.il

A. Galperin
Ben-Gurion University of the Negev, alexg@bgu.ac.il

E. Shwageraus
Ben-Gurion University of the Negev, eush@bgu.ac.il

Dissolution, Reactor, and Environmental Behavior of ZrO_2-MgO Inert Fuel Matrix

Neutronic Evaluation of MgO-ZrO_2 Inert Fuels

Final Report

Prepared by Reactor Analysis Group

Department of Nuclear Engineering

Ben-Gurion University of the Negev

Beer-Sheva, Israel

July 2006

E. Fridman, A. Galperin, E. Shwageraus

Table of Contents

List of Figures

List of Tables

Executive Summary

In the second year of the "Dissolution, Reactor, and Environmental Behavior of ZrO_2-MgO Inert Fuel Matrix" project initiated and directed by UNLV, the Ben-Gurion University (BGU) group research was focused on the development of practical PWR core nuclear design fully loaded with Reactor Grade (RG) Pu fuel incorporated in fertile free matrix. The design strategy was based on the basic feasibility study results performed at BGU in the Year 1 of the project.
In the Year 2 of the project, the BGU work consisted of the following research tasks:

Reference Core 3D Analysis

Three-dimensional full core model was developed for two reference cases to assess the performance of calculational tools (ELCOS system [1]) and as a basis for comparison.

1. Standard PWR core with conventional all-UO_2 fuel, 18 calendar month fuel cycle.
2. Full fertile free RG-Pu loaded PWR core, 12 months fuel cycle. The model is based on the analysis performed at PSI and reported in Reference [2].

The basic set of most important neutronic characteristics was calculated with the developed core model.

The results obtained in this task were compared with those reported in Reference [2]. Very good agreement was observed in all parameters available for comparison: critical boron letdown curve, power peaking factors, and actinides mass balances. The existence of small differences was attributed to the uncertainty in some of the model parameters not published in Reference [2] e.g. radial and axial fuel burnup distributions of the equilibrium core.

Selection BP Designs

Three most promising burnable poison designs were selected for further analysis based on the previous year results. The designs include a combination of different burnable poison materials and configurations to address all the FFF design issues. The three design options considered for 3-D analysis are:
- combination of homogeneously mixed Er with Hf-IFBA coating

- combination of homogeneously mixed Hf with Er-IFBA coating
- homogeneously mixed Er enriched in Er-167 isotope.

These options were found to be a reasonable compromise in terms of operational core characteristics; namely, cycle penalty, maximum critical boron concentration, and acceptable reactivity coefficients.

Adaptation of the Available Simulation Tools to Handle Fertile Free Fuel Calculations

The three-dimensional nodal diffusion code SILWER, which is a part of the ELCOS system, was originally developed for simulation of conventional LWR fuel. In this part of the project, thermal-hydraulic feedback module of the SILWER code was extended to allow analysis of non-uranium fuels and annular pellet geometries.

The modification was shown to have a significant effect on the accuracy of calculations. The use of appropriate thermal conductivity data results in appreciable difference in fuel temperature distribution compared with the results that are based on the default UO_2 thermal conductivity data. The correct calculation of the fuel temperature, in turn, leads to more accurate estimation of Doppler Effect and therefore more accurate calculation of critical boron concentration and fuel cycle length.

Full Core Analysis of the Selected BP Options and Assessment of Reactivity Coefficients

Three-dimensional full core simulations of the selected BP options including thermal-hydraulic feedback were performed in this task.

The objective was to calculate major core performance parameters, reactivity feedback coefficients and fuel temperature distribution for FFF cores and compare these parameters with those of the reference all-UO_2 and all-FFF (PSI design) cores.

The calculations were performed with SILWER computer code, which was modified to allow treatment of non-UO_2 fuels and annular fuel pellets in the fuel temperature calculation module. A standard 3400MW PWR core was used as reference for the calculations.

Three burnable poison design options were considered:

- Hf Homogeneously mixed with fuel – Er IFBA coating – Boron WABA
- Er Homogeneously mixed with fuel – Hf IFBA coating – Boron WABA
- Enriched Er Homogeneously mixed with fuel

The results of the analysis show that the use of all three burnable poison options is potentially feasible. All major core performance parameters for the analyzed cases are very close to those of a standard PWR with conventional UO_2 fuel including possibility of reactivity control, power peaking factors, and cycle length.

Among the three analyzed BP design options for the fertile free MgO-ZrO_2 matrix fuel, the Enriched Er option was shown to be the most effective one with respect to the minimal cycle length penalty and efficiency of Pu destruction. This advantage has to be evaluated carefully against considerable costs associated with Er enrichment. The additional two BP options considered in this study exhibit similar performance.

The MTC of all FFF cores is negative at the full power conditions at all times and very close to that of the UO_2 core.

The Doppler coefficient of the FFF cores is also negative but somewhat lower in magnitude compared to UO_2 core. The significance of such difference can only be assessed in a comprehensive analysis of all relevant reactor transients in which Doppler feedback is of major importance. The Homogeneously mixed Hf – IFBA Er design shows a slight advantage in terms of the more negative Doppler Coefficient over the rest of the FFF core designs.

The soluble boron worth of the FFF cores was calculated to be lower than that of the UO_2 core by about a factor of two, which still allows the core reactivity control with acceptable soluble boron

concentrations. The lower control rod worth may represent a potential design problem of inadequate shutdown margin. This problem can be addressed either by using extra control rods in the Full-MOX PWRs or by using control rods with enriched boron.

The steady state fuel temperature distributions in FFF cores are also similar to the reference UO_2 core. In the FFF core, the core average fuel temperature is lower than that of the UO_2 core by about 100°C due to the higher thermal conductivity of the MgO-ZrO_2 matrix. However, the maximum fuel temperatures in the hot assemblies in the FFF and the UO_2 cores are very close because of the slightly higher power peaking in the FFF cores which cancels out the effect of the better thermal conductivity.

In summary, the results of the analysis show that the FFF cores with all three considered burnable poison options are potentially feasible. The conclusion is based on the fact that all calculated FFF core performance characteristics are close to those of the reference PWR core with conventional UO_2 fuel. This study had shown that the FFF core characteristics are adequate for the steady state reactor operation.

Further detailed analysis should be performed to ensure the FFF core safety also under accident conditions. Such analysis should take into account the whole spectrum of thermal, mechanical, and neutronic characteristics of the fertile free fuel and therefore is beyond the scope of this project.

I. Task 1: Reference Core 3D Analysis

This part of the report summarizes the results of the calculations performed on Task 1 of the Year 2 BGU program. In this task, three-dimensional simulations of two reference cores were performed. These reference cases are:

- Standard PWR core with conventional all-UO2 fuel, 18 calendar month fuel cycle.
- Full fertile free RG-Pu loaded PWR core, 12 month fuel cycle. This model is based on the analysis performed at PSI [2].

The results of 3D calculations of reference cores will provide the basis for the consistent comparison of the future FFF cores designs. The analysis addressed the following core characteristics:

- Core loading.
- Critical soluble boron concentration.
- Power peaking factors.
- For fertile free core: BOL and EOL concentration of Pu and MA.
- Reactivity coefficients.
- Fuel temperature.

It should be noted that calculation of reactivity coefficients and fuel temperature require certain modification in the core 3D core simulation code SILWER. Therefore, these two groups of parameters will be reported in the Task 2.

I.1 Analysis Methodology

All reactor physics calculations, presented in this task were performed with the ELCOS [1] code system, which was developed for static simulations of Pressurized and Boiling Water Reactors. ELCOS consists of the following four computer codes:

- ETOBOX code generates a group-wise (respectively point-wise in the resonance range) cross-section library from a basic library in ENDF/B-format.
- BOXER code performs cell and two-dimensional transport and depletion calculations. It produces state variable dependant cross section library for 3D full core simulations.

- CORCOD code computes interpolation coefficients based on the BOXER results. These coefficients are later used in the three-dimensional calculations.
- SILWER code performs three-dimensional neutronic calculations with thermal hydraulic feedbacks of the reactor core.

ELCOS is written in FORTRAN-77. The use of direct access files, as well as the dynamic memory allocation, results in short running times even for complex problems. The structure of ELCOS is schematically presented in Figure I-1. The coupling of the codes to each other is shown along with the most important files.

I.1.1 ETOBOX: Cross section library processing

ETOBOX [3] allows handling of the data in ENDF/B format (up to ENDF/B-5) and produces a cross section library for the BOXER code. Continuous cross sections are collapsed into energy groups. The scattering matrices (elastic, inelastic and (n,xn) reactions) are calculated for a given order of anisotropy (presently P_0 and P_1, with P_2 transport correction for the elastic scattering). In the so called resonance range (between 1.3 and 907 eV), the resonance parameters are transformed into pointwise lists for different temperatures. Above 907 eV the resonance cross sections are integrated into groups for different temperatures and the dilution cross section. In the thermal energy range, the scattering matrices are calculated through integration of the $S(\alpha,\beta)$-matrices from ENDF/B, or by means of the free gas model.

The structure of the present library is based on 70 energy groups with the thermal cutoff at 1.3 eV. The library contains 162 nuclides or mixtures. Most of them are taken from JEF-1, the erbium isotopes come from the Russian file BROND-2, and Gd-155 from the Japanese file JENDL-2.

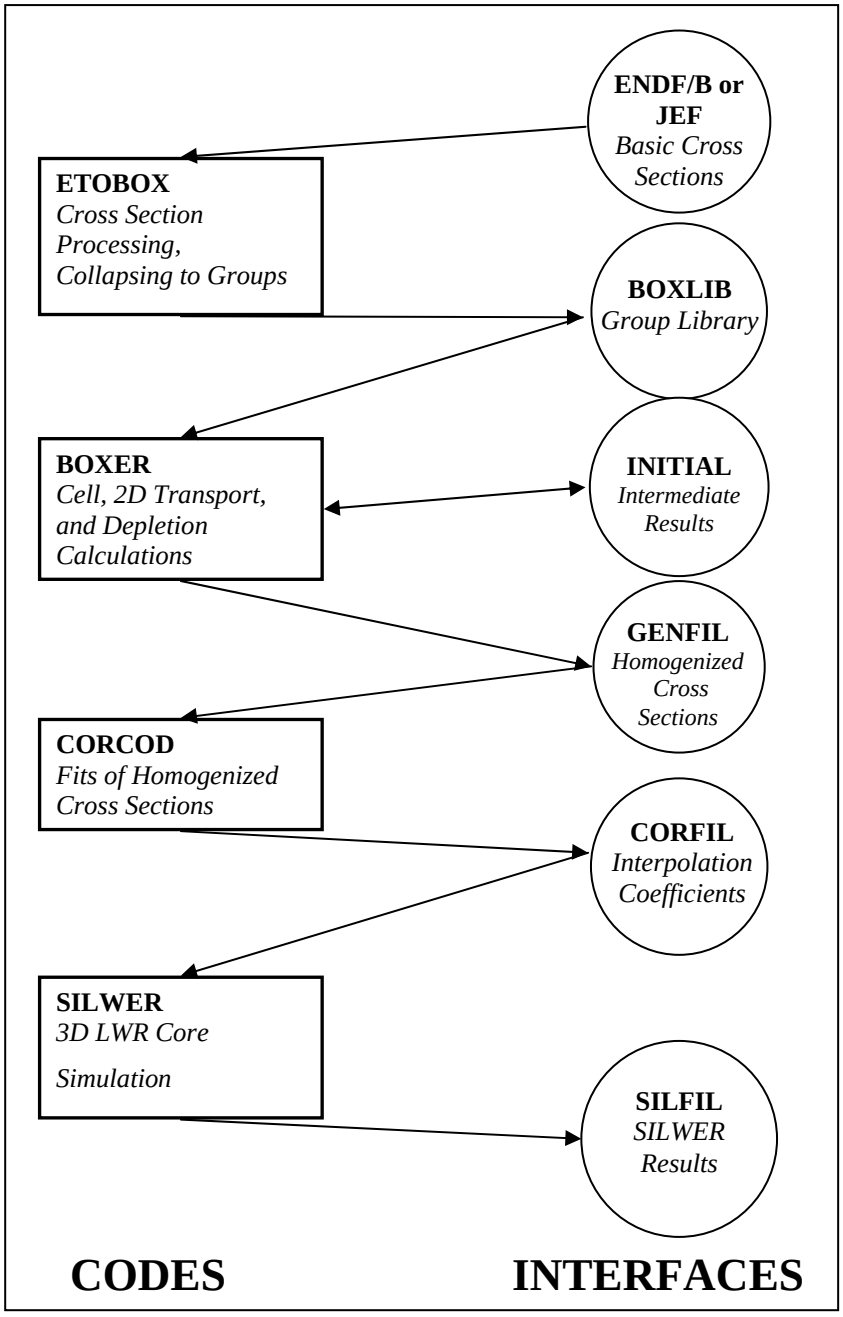

Figure I-1. ELCOS code system overview

I.1.2 BOXER: Unit cell and 2D lattice calculations

BOXER [4] is a modular code for two-dimensional calculation of LWR fuel assemblies. The main modules of the code are:

Cell calculation:

In every configuration to be treated, the most important cell from the point of view of the neutron spectrum is chosen as the "principal cell type". It is calculated with white boundary conditions. Its outgoing partial currents can be used as boundary conditions for other cell types and for the homogeneous materials. The cell calculation begins with the resonance calculation in two material zones and about 8000 lethargy points depending on the composition of the material, employing collision probability method. The resulting ultra fine spectrum is used as weighting function to condense the point-wise cross sections into groups. Afterwards, a one-dimensional flux calculation is done with a transport theory in cylindrical or slab geometry and in 70 energy groups, in all zones of the cell. Then the cross sections of the cell are condensed spatially as well as energetically.

Two-dimensional modules:

The configuration is represented by a X-Y mesh grid. The flux distribution can be calculated by either diffusion or a transport module. The results are the multiplication factor - keff, neutron flux, power distribution, and reaction rates. A spatial and energetic condensation of the group constants produces the input data for the correlation code CORCOD.

Burnup:

The evolution of isotopic densities for each material is calculated using reaction rates collapsed to one group by weighting with the multigroup fluxes from the cell- and the two-dimensional calculations. The time dependence of the nuclide densities is described by Taylor series. The nuclide densities with high destruction rates are assumed to be asymptotic. An iterative correction adjusts the fluxes within the time step in order to keep the power constant. The effect of the changing spectrum on the reaction rates is taken into account by a predictor-corrector method and by density dependent one-group cross sections within the time step for ^{239}Pu and ^{240}Pu

(approximated by a rational function). In the predictor-corrector method, the depletion is performed twice – using the spectrum at the beginning and at the end of the timestep. Average isotope number densities between these two calculations are then used as initial values for the subsequent burnup step. A time step can be divided into several micro-steps without recalculating the reaction rates in order to improve the numerical accuracy of the depletion calculation.

Decay:

The DECAY option may be used to modify the isotopic densities due to radioactive decay in all fuel materials.

I.1.3 CORCOD [5]: Correlation code

The results obtained from the BOXER (condensed group constants, k-eff, etc.) are represented as polynomials of independent state variables. These variables are: power density, burnup, actual and burnup weighted water density, water and fuel temperature, soluble boron concentration and ^{135}Xe density. The coefficients of the polynomials constitute the data library for the 3D code SILWER. For each state variable, the maximum order can be given by input. The coefficients are determined by the least squares fit method or by statistical method which automatically suppresses terms of lower importance. The list of the terms can also be modified through the input.

I.1.4 SILWER: Three-dimensional LWR simulation code

This code simulates an LWR core in steady state operation. A typical configuration consists of the active core with its reflectors. The code calculates the multiplication factor k-eff, spatial power distribution, burnup, neutron flux, water density and temperatures of the fuel, clad and water. Critical condition search can be performed for the k-eff eigenvalue, control rods position or boron concentration. The main modules of the SILWER are:

Neutronic module: The multiplication factor, flux and spatial power distribution can be calculated with two different nodal diffusion modules, one with polynomial expansion and the other with analytical solutions of the diffusion equation in each node.

Thermal hydraulics: SILWER has two thermal hydraulic modules, one for pressurized water reactors (PWR) and the other for boiling water reactors (BWR). The calculated characteristics are the void fraction, pressure drop, distribution of the mass flow, water temperature and density, and temperature distributions in fuel and clad.

Local power density: The local pin by pin power density distribution in each node can be calculated with the PINPOW module.

Interpolation of the group constants: The interpolation is done for each node of the configuration on the basis of the interpolation coefficients from CORCOD.
The system state variables (power distribution, thermal hydraulics, control rods position) are evaluated iteratively. The burnup distribution is calculated through integration over a time step assuming a constant value of the system variables during the time step.

I.2 Reference cores parameters

Reference All-UO_2 PWR core

A standard 4-loop Westinghouse PWR was selected as a reference all-UO2 case for this study. The fuel type is a 17×17 fuel assembly with 116 IFBA type BP pins. The fuel assembly and core parameters, as well as the reactor core operating conditions used in the calculations are summarized in

Table I-1. The fuel assembly configuration is presented in Figure I-2.

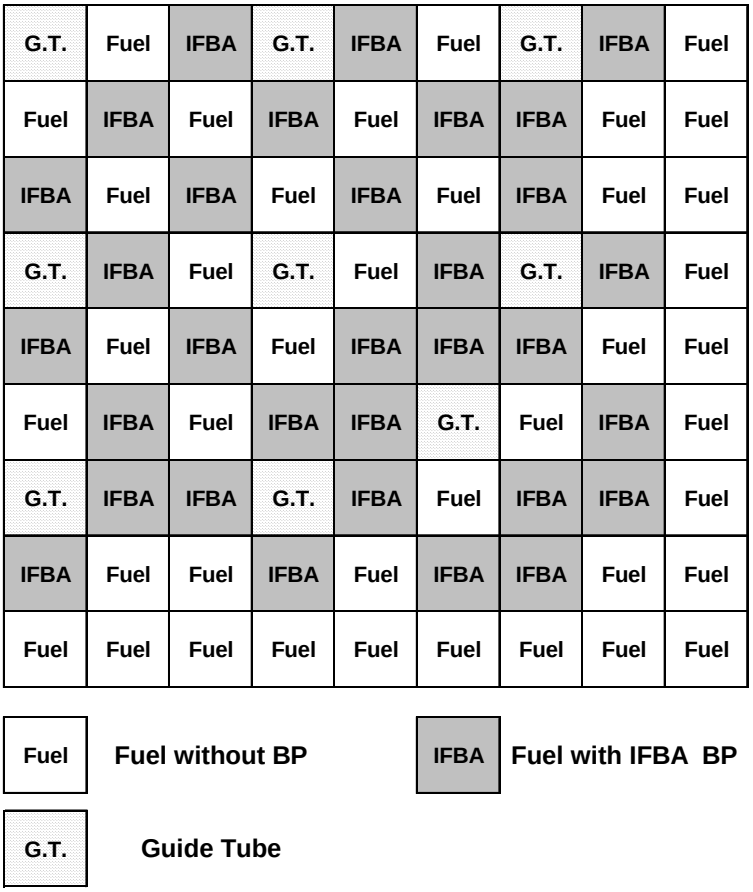

Figure I-2. UO_2 fuel assembly with 116 IFBA pins

Table I-1: Parameters of the reference all-UO_2 core

Operating parameter	Value
Core	
Total thermal output (MWth)	3358
Number of fuel assemblies in the core	193
Average core power density (MW/MTHM)	37.3
System pressure (bar)	155
Total core flow rate (kg/s)	18600
Core inlet temperature (ºC)	289.1
Fuel Assembly	
Active fuel height (cm)	366
Assembly array	17 × 17 pins
Total number of fuel rods per assembly	264
Number of IFBA rods per assembly	116
Number of grids per assembly	7
Assembly pitch (cm)	21.5
Assembly gap (cm)	0.08
Fuel rod pitch, cm	1.26
Number of guide tubes	25
Guide tube inner radius (cm)	0.5715
Guide tube outer radius (cm)	0.6120
Fuel Rod	
Cladding outer radius (cm)	0.4750
Cladding thickness (cm)	0.0570
Cladding material	Zircaloy
Fuel Pellet	
Fuel material	UO_2
Fuel enrichment (w/o of U235)	4.21
Fuel pellet radius (cm)	0.4095
IFBA coating thickness (mm)	0.0105
IFBA Burnable poison	
BP material	ZrB2
BP loading (mg/cm of B10)	0.62

I.3 Reference 100%-FFF PWR core

Currently, there is no industrial experience with fertile free fuel use in commercial PWRs, so that no measured data exists on the neutronic parameters of fertile free cores. However, a comprehensive study was done at Paul Scherrer Institute (PSI) in Switzerland, which modeled various fertile free cores and compared their neutronic characteristics with the conventional UO_2 core [2].

The reference reactor, used in the study reported in Reference 2, was assumed to be operating in 300 EFPD cycle with 4-batch fuel management. Therefore, the initial Pu and burnable poison loadings should presumably be much lower than those required for the operation of typical US PWR with 18 calendar months cycle and 3-batch fuel management. Moreover, the 4-batch core is much more flexible in leveling the core radial power profile than the 3-batch core. As a result, the conclusions reported in Reference 2 cannot be applied directly to the typical US PWR (18 months cycle, 3-batch core). However, the Reference 2 results can be used to assess the capabilities of the computational tools available for the current analysis, which is the second objective of the 2nd year Task 1. The main parameters of the 100%-FFF core taken from the Reference 2 are presented in

Table I-2.

Table I-2: Parameters of the reference 100%-FFF core

Operating parameter	Value	
Core		
Total thermal output (MWth)	3000	
Number of fuel assemblies in the core	177	
Average core power density (MW/m^3)	103.0	
System pressure (bar)	154	
Total core flow rate (kg/s)	15665	
Core inlet temperature (ºC)	291.5	
Fuel Assembly		
Active fuel height (cm)	359.5	
Assembly array	15 × 15 pins	
Total number of fuel rods per assembly	205	
Number of grids per assembly	7*	
Assembly pitch (cm)	21.56	
Assembly gap (cm)		
Fuel rod pitch, cm	1.43	
Number of guide tubes	20	
Guide tube inner radius (cm)	0.5715*	
Guide tube outer radius (cm)	0.6120*	
Fuel Rod		
Cladding outer radius (cm)	0.5375	
Cladding thickness (cm)	0.0725	
Cladding material	Zircaloy	
Annular Fuel Pellet		
Fuel material	Mixture of RG PuO2, ZrO2 and Er2O3	
Material composition (g/cm^3)	Pu	1.2
	Er	0.4
	O	0.24
	ZrO2	5.44
Pu vector (w/o)	Pu238	2.7
	Pu239	54.5
	Pu240	22.8
	Pu241	11.7
	Pu242	8.3
Central pellet region material	Reduced density (5.2 g/cm^3) ZrO2	
Fuel pellet inner radius (cm)	0.45650	
Fuel pellet outer radius (cm)	0.22825	
* Unavailable from Ref. 2		

I.4 Reference cores performance parameters

This section presents the results of the full core simulations in three dimensions of all-UO2 and 100%-FFF cores. The results of 100%-FFF core simulation were compared with those available from Ref. 2. The analysis addressed the following core characteristics:

- In-core fuel management scheme.
- Critical soluble boron concentration.
- Power peaking factors.
- For fertile free core: BOL and EOL concentration of Pu and MA.

It should be noted that investigation and analysis of the reactivity coefficients will be performed in the Task 2. Table I-3 presents designations for all cores under consideration.

Table I-3: Description of considered cases

Case designation	Case description
BGU-UO2	Reference All-UO_2 PWR core calculated at BGU
BGU-FFF	Reference All-FFF PWR core calculated at BGU
PSI-FFF	Reference All-FFF PWR core calculated at PSI (From [2])

I.5 In-core fuel management scheme

A 3-batch in-core fuel management scheme was adopted for all-UO_2 core. In BGU-FFF core the fuel was managed in four-batch mode as mentioned earlier. The fissile loadings of the fuel were adjusted to achieve fuel cycle length of 18 calendar months for all-UO_2 core. In the FFF core cases the Pu loading was taken as reported in Reference 2.

First BGU-UO2 core was loaded with 3 fuel batches at 3 different exposure levels of 0, BU1, and 2·BU1, where BU1 is the average target core burnup at EOC providing the fuel cycle length of 18 months. For the following cycles, the BOC exposure levels of once burned and twice burned batches were taken to be equal to the previous core average EOC exposure levels of fresh and once burned batches respectively. Following three transitional cycles, an equilibrium loading patterns with a typical low-leakage configuration were established for BGU-UO_2 core. In such a

configuration, the once-burned fuel assemblies are placed in the core periphery to reduce the core leakage and neutron fluence to the pressure vessel, while fresh and twice-burned fuels are arranged in a checkerboard pattern as shown in Figure I-3.

The equilibrium BGU-FFF core was simulated in a similar to BGU-UO_2 core manner except for the fact that 4 batches at 4 different exposure levels were used. The loading pattern for BGU-FFF core was adopted from the Ref. 2 and shown in Figure I-4.

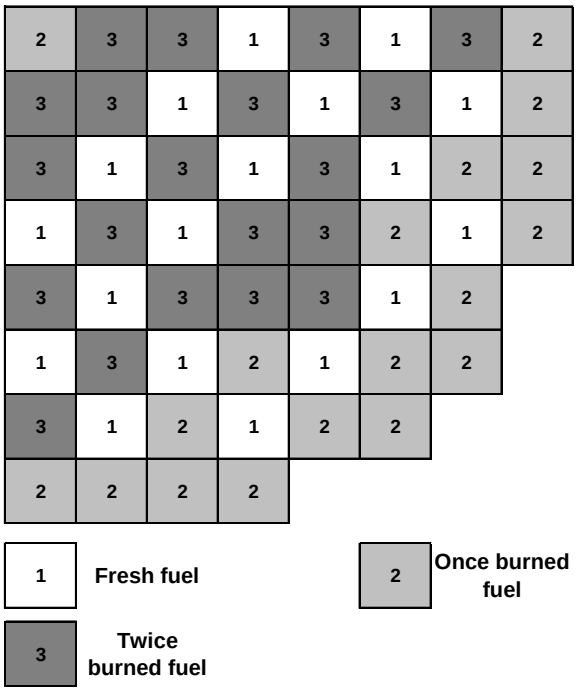

Figure I-3. BGU-UO_2 core fuel loading map

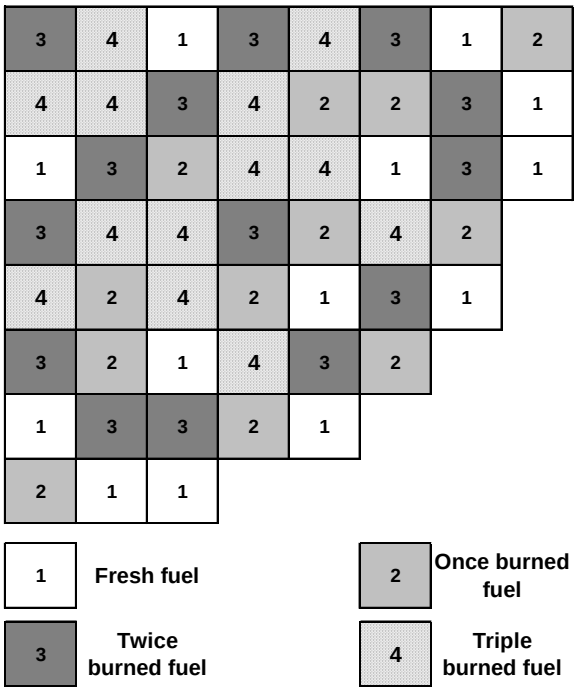

Figure I-4. BGU-FFF core fuel loading map

I.6 Critical soluble boron concentration and cycle burnup

Figure I-5 shows the critical soluble boron concentration (CBC) vs. core depletion time for all considered cases. There is a good agreement between PSI-FFF and BGU-FFF critical boron let down curves. A slight difference of about 30 ppm of CBC at BOC is most likely due to the fact that the exact axial and radial burnup distributions of the equilibrium core were not available from the Reference 2. The equilibrium cycle lengths were found to be equal to 436 EFPD for the BGU-UO2 core, 313 EFPD for the BGU-FFF core, and 306 EFPD for the PSI-FFF core. The BU maps for equilibrium BGU-UO2 and BGU-FFF cores are shown in Figure I-6 and

Figure I-7 respectively. Table I-4 summarizes the batch average BOC and EOC burnup levels for all calculated cases.

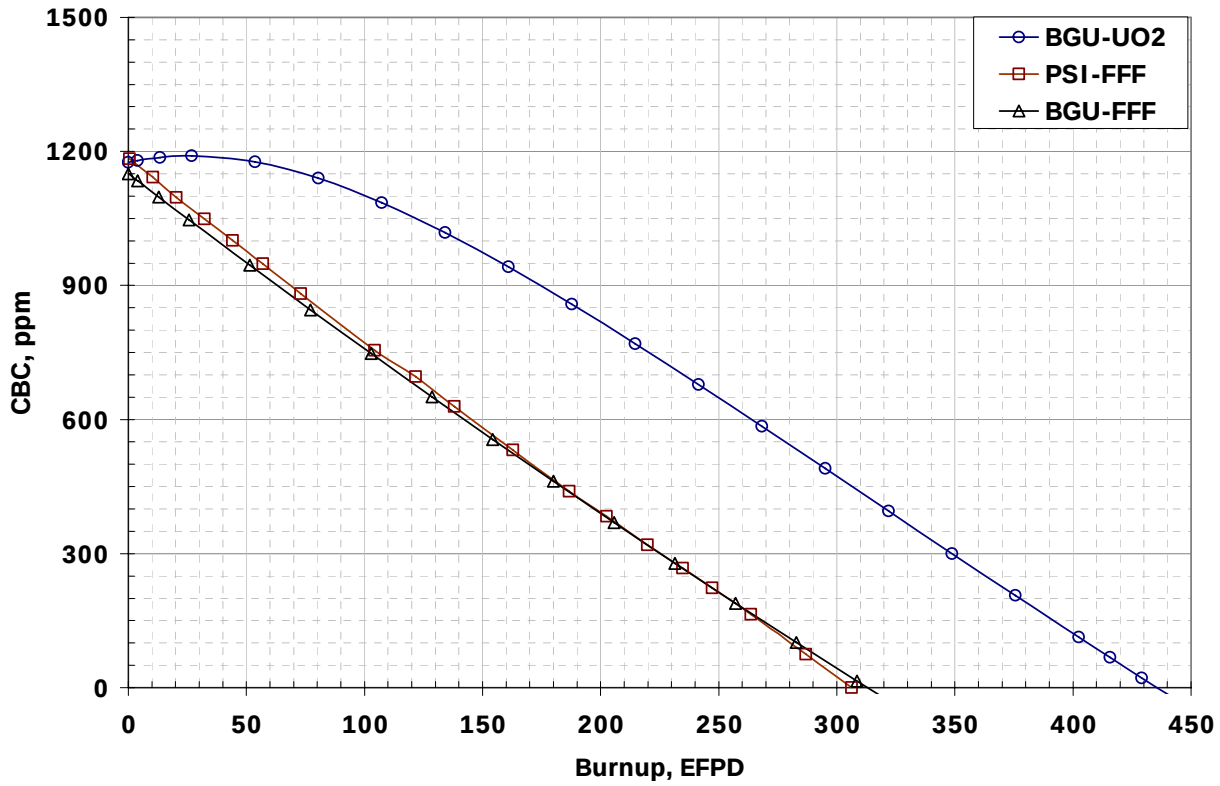

Figure I-5: Critical boron concentration for three cores under consideration.

20999 34810	32420 45690	32420 48530	0 23260	32420 50430	0 22510	32420 46860	20999 30680
32420 45690	32420 47010	0 21960	32420 50070	0 23260	32420 49560	0 19520	20999 30990
32420 48530	0 21960	32420 49590	0 22160	32420 48730	0 22020	20999 37310	20999 30510
0 23260	32420 50070	0 22160	32420 47300	32420 46470	20999 38120	0 17490	20999 28760
32420 50430	0 23260	32420 48730	32420 46470	32420 46250	0 18430	20999 32280	
0 22510	32420 49560	0 22020	20999 38120	0 18430	20999 33420	20999 27940	
32420 46860	0 19520	20999 37310	0 17490	20999 32280	20999 27940		
20999 30680	20999 30990	20999 30510	20999 28760	<BOC <EOC			

Figure I-6: BOC and EOC burnup map for BGU-UO_2 equilibrium core

234864 363100	384330 500300	0 158300	234864 379400	384330 512400	234864 386500	0 151100	107585 198600
384330 500300	384330 503400	234864 376400	384330 507100	107585 263700	107585 266400	234864 364500	0 88600
0 158300	234864 376400	107585 257300	384330 504800	384330 506100	0 152600	234864 344900	0 66380
234864 379400	384330 507100	384330 504800	234864 375300	107585 254500	384330 488400	107585 195000	
384330 512400	107585 263700	384330 506100	107585 254500	0 142100	234864 333200	0 59300	
234864 386500	107585 266400	0 152600	384330 488400	234864 333200	107585 174200		
0 151100	234864 364500	234864 344900	107585 195000	0 59300			
107585 198600	0 88600	0 66380	<BOC <EOC				

Figure I-7: BOC and EOC burnup map for BGU-FFF equilibrium core

Table I-4: BOC and EOC batch average burnup summary

		Fresh	Once	Twice	Triple
BGU-UO_2	**BOC**	0	20999	32420	N/A
	EOC	20966	32284	48208	N/A
BGU-FFF	**BOC**	0	107585	234864	384330
	EOC	107751	235391	369998	502627

I.7 Power peaking factors

The radial and axial power distributions were tracked for BGU calculated cores and presented in Figures I-8 through I-11. The power profile data was not available from the Reference 2. Therefore, only maximum values of the power peaking factors of the FFF core are compared with those calculated at PSI. The comparison is presented in

Table I-5. The difference in the prediction of power peaking factors does not exceed 5% and most likely originating from the fact that the initial radial and axial burnup distributions were not available.

Table I-5: Summary of power peaking factors

	BOC		EOC	
	Radial Peak	**Axial Peak (Core Ave.)**	**Radial Peak**	**Axial Peak (Core Ave.)**
PSI-FFF	1.38	1.20	1.40	1.22
BGU-FFF	1.39	1.19	1.33	1.19
BGU-UO_2	1.49	1.22	1.25	1.15

1.005 0.842	0.936 0.821	1.102 0.943	1.494 1.232	1.196 1.033	1.376 1.24	0.89 0.903	0.578 0.624
0.936 0.821	1.01 0.879	1.417 1.187	1.189 1.013	1.464 1.252	1.101 1.025	1.146 1.131	0.595 0.64
1.102 0.943	1.417 1.187	1.157 0.997	1.407 1.21	1.076 0.981	1.343 1.251	1.021 0.997	0.564 0.618
1.494 1.232	1.189 1.013	1.407 1.21	0.991 0.918	0.92 0.902	1.091 1.06	0.992 1.059	0.438 0.524
1.196 1.033	1.464 1.252	1.076 0.981	0.92 0.902	0.866 0.922	1.048 1.145	0.647 0.753	
1.376 1.24	1.101 1.025	1.343 1.251	1.091 1.06	1.048 1.145	0.72 0.834	0.382 0.493	
0.89 0.903	1.146 1.131	1.021 0.997	0.992 1.059	0.647 0.753	0.382 0.493		
0.578 0.624	0.595 0.64	0.564 0.618	0.438 0.524	<BOC <EOC			

Figure I-8: Normalized radial power density for BGU-UO_2 core at BOC and EOC

(see Figure I-3 for batch designation)

1.143 0.989	1.053 0.87	1.389 1.25	1.262 1.13	1.125 0.982	1.266 1.238	1.218 1.305	0.704 0.825
1.053 0.87	1.077 0.894	1.245 1.099	1.094 0.932	1.32 1.27	1.309 1.327	1.043 1.107	0.685 0.807
1.389 1.25	1.245 1.099	1.295 1.19	1.061 0.926	1.053 0.955	1.249 1.301	0.872 0.961	0.503 0.622
1.262 1.13	1.094 0.932	1.061 0.926	1.188 1.137	1.207 1.238	0.851 0.872	0.671 0.8	
1.125 0.982	1.32 1.27	1.053 0.955	1.207 1.238	1.144 1.234	0.766 0.876	0.445 0.563	
1.266 1.238	1.309 1.327	1.249 1.301	0.851 0.872	0.766 0.876	0.496 0.633		
1.218 1.305	1.043 1.107	0.872 0.961	0.671 0.8	0.445 0.563			
0.704 0.825	0.685 0.807	0.503 0.622	<BOC <EOC				

Figure I-9: Normalized radial power density for BGU-FFF core at BOC and EOC

(see Figure I-4 for batch designation)

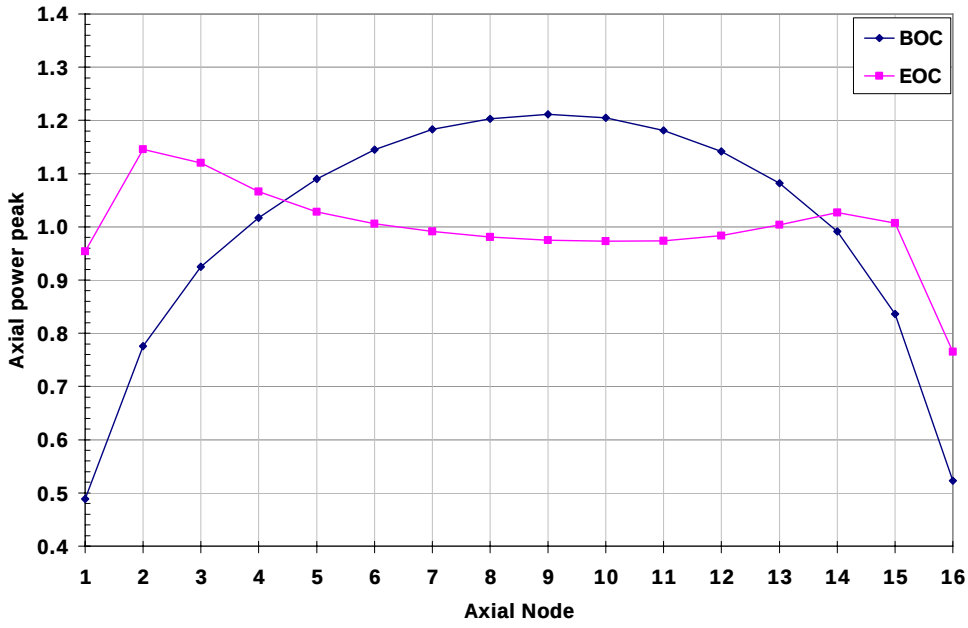

Figure I-10: Core average axial power profile: BGU-UO_2 case

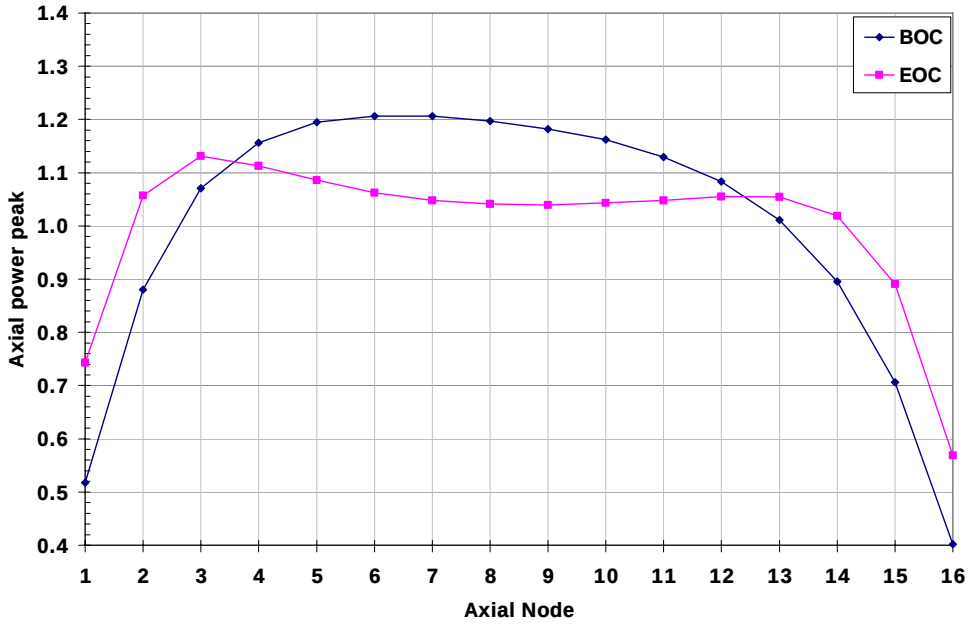

Figure I-11: Core average axial power profile: BGU-FFF case

I.8 Actinides Mass Balance

Table I-6 compares concentrations of Pu and most neutronically important MA at BOC and EOC for the BGU-FFF and PSI-FFF cores. Table I-6 shows that nearly 60% of total initial Pu can be incinerated utilizing fertile free fuel in the proposed core configuration. A minor difference in the concentrations at EOC can be, again, attributed to the lack of data in the PSI core model description.

Table I-6: Concentrations of Pu and MA at BOL and EOL for BGU-FFF and PSI-FFF cores (relative to initial Pu mass).

	BOC		**EOC**	
	BGU-FFF	**PSI-FFF**	**BGU-FFF**	**PSI-FFF**
Pu238	2.7%	2.7%	2.0%	2.0%
Pu239	54.5%	54.5%	6.6%	6.5%
Pu240	22.8%	22.8%	15.2%	15.1%
Pu241	11.7%	11.7%	8.8%	9.1%
Pu242	8.3%	8.3%	10.3%	10.2%
Total Pu	**100%**	**100%**	**42.9%**	**42.9%**
Am241	0.00%	0.00%	0.70%	0.71%
Am243	0.00%	0.00%	2.34%	2.22%
Cm242	0.00%	0.00%	0.24%	0.23%
Cm244	0.00%	0.00%	1.59%	1.55%
Cm245	0.00%	0.00%	0.18%	0.18%
Total MA	**0.00%**	**0.00%**	**5.05%**	**4.89%**

I.9 Summary and Conclusions

In this task, two different PWR cores were modeled with ELCOS computer code system.

First, the model for standard 4-Loop 3358 MW_{th} PWR loaded with standard UO_2 fuel assemblies operating at 18 calendar months power cycle was developed. The basic set of most important neutronic characteristics was calculated with the developed core model. This set of parameters will serve as a basis for comparison with fertile free fuel core designs to be developed in the next tasks.

Second, the existing fertile free core design reported in Reference [2] was evaluated independently in order to confirm the available core modeling tools capabilities. The results obtained in this task were compared with those reported in Reference [2]. Very good agreement was observed in all parameters available for comparison: critical boron letdown curve, power peaking factors, and actinides mass balances. The existence of small differences was attributed to the uncertainty in some of the model parameters not published in Reference [2] e.g. radial and axial fuel burnup distributions of the equilibrium core.

II. Task 2: Summary and Discussion of Impact of Analyzed BP Designs and Selection of BP options for 3D full core analysis

This section of the report presents summary of the results obtained for several BP design options. The design options shown in Table II-1 were selected based on their impact on core performance parameters:

- Reduction of required critical boron concentration (CBC),
- Doppler Coefficient (DC),
- Moderator Temperature Coefficient (MTC),
- Residual reactivity penalty, in effective full power days (EFPD), and
- Soluble Boron Worth (BW).

The performance parameters were compared with those of a reference all-U assembly with Uranium enrichment of 4.21%, required to achieve a 18-month cycle length for a 3-batch fuel management scheme.

The results, obtained by a series of assembly (2D) calculations and an application of a modified linear reactivity model and described in final report for Task 1 of the current project [1], were grouped by a specific BP material: Gd, Hf, and Er. For each BP material three geometrical arrangements were considered: WABA, IFBA, and Homogeneous Fuel/BP mixture.

The impact of different BP designs may be now summarized in following observations:

1. No-BP lattice demonstrates unacceptably high CBC at beginning of cycle (BOC) of about 5,000 ppm and almost zero value of MTC at BOC. DC is reduced by a factor of 2 during the burnup cycle. BW is reduced by more than a factor of 2 at BOC and is improving with burnup.
2. Observation points listed in item 1 indicate that the main attention should be focused towards improving the performance parameters at BOC.

3. The main limiting performance parameter for the assessment of a specific design is clearly the maximum required CBC. With a reasonable assumption that the maximum CBC will occur at BOC, the results are commented in the following item.
4. A single BP design capable of CBC reduction around or lower than 2,000 ppm without considerable fuel cycle length penalty is Homo-Gd (case #30 in the previous task final report [1]). However, this BP option results in a strongly positive MTC and is, therefore, rejected as a single BP option.
5. Observation of the CBC Max. column indicates that NO single BP design is capable to produce required reactivity related performance with a reasonable cycle length penalty. **Therefore, the continuing design effort of the present study will be mainly focused on a combination of two BP designs**.
6. Homogeneous designs for Hf and Er result in max. CBC in the range of 2,400 – 2,600 ppm, thus indicating a possible utilization as one of the components of a 2-BP design. It should be noted that, due to a heavy BP loading (typical for a homogeneous fuel/BP mixture), those options designs show a significant cycle penalty of 40 – 100 EFPD's.
7. With regard to DC, it may be noted that WABA-type designs have no impact, while IFBA-type designs for Er and Hf cause a modest improvement on this parameter. A significant improvement of the DC may be achieved by a heavy loading of Hf or Er as a homogeneous option, with the disadvantage of cycle penalty, mentioned above.

Keeping in mind that the main objective of the present study is to assess the viability of the full core FFF design by judicious application of the burnable poisons, the following guidelines are formulated:

The design objectives and constraints adopted are:

- Maximum critical boron concentration for burnup-related reactivity control does not exceed 2,000 ppm, and
- Moderator Temperature Coefficient is negative during the power production cycle.
- More negative value of Fuel Temperature Coefficient (DC).
- Minimization of reactivity penalty (expressed in EFPD's),

Table II-1: Summary of Results for Selected BP Design Options

Case No.	Case Designation	CBC BOC, ppm	CBC Max, ppm	Cycle penalty, EFPD	DC, pcm/˚C		MTC, pcm/˚C		BW, pcm/ppm	
					BOL	EOL	BOL	EOL	BOC	EOC
Ref.	UO_2, e=4.21%				-2.0	-3.4	11.2	-59.9	-5.8	-9.5
1	No BP	4856	4856	0	-1.0	-1.5	0.61	-27.0	-2.4	-15.3
13	WABA-Gd-9	3473	3473	67	-1.0	-1.6	-20.7	-39.6	-2.2	-12.9
25	IFBA-Gd-4	598	2397	6	-0.9	-1.5	96.9	-32.6	-1.8	-14.9
30	HOMO-Gd-3	N/A	1117	16	-1.0	-1.5	120.7	-32.0	-1.8	-15.5
16	WABA-Hf-3	3818	3818	51	-1.0	-1.8	-17.3	-60.8	-2.2	-13.8
26	IFBA-Hf-1	3486	3486	43	-1.2	-1.6	-9.7	-40.0	-2.5	-15.4
37	HOMO-Hf-1	2425	2425	101	-1.6	-2.0	-18.8	-43.8	-2.6	-14.9
19	WABA-Er-3	3787	3787	47	-1.1	-1.8	-12.6	-53.2	-2.2	-13.3
27	IFBA-Er-1	3789	3789	16	-1.1	-1.5	-7.0	-34.9	-2.5	-19.0
46	HOMO-Er-1	2604	2604	41	-1.3	-1.5	-13.2	-37.8	-2.6	-14.8

Following the reasoning presented in a list of observations above, two possible directions were adopted for selection of the optimal BP design options: 1) combination of two BP designs, and 2) utilization of an enriched BP material. The first direction presents an attempt to combine the beneficial effects of different BP designs, and the second direction aimed to "improve" the isotopic composition of a selected BP material.

Six additional cases were formulated accordingly: combinations of Homo-Hf with IFBA-Er, combination of Homo-Er with IFBA-Hf and finally two single BP materials designs based on enriched Er homogeneously mixed with fuel. All design options were based on maximum amounts of BP loaded: all fuel rods include homogeneously mixed BP and IFBA BP ring.

The results of the calculations are shown in Table II-2. Enriched Er composition, with abundance of Er-167 arbitrarily increased to 80% and all remaining isotopes abundance re-normalized following the ratios of natural Er, is shown in Table II-3.

Figures II-1 and II-2 present the fuel assembly criticality and the core critical boron concentration respectively for the combined WABA-Gd and IFBA-Er design. These designs may also be considered for the 3D neutronic simulations since the impact of WABA removal from the core are difficult to assess based on the 2D calculations.

The results summarized in Table II-2 and Figures II-3 and II-4 demonstrate that all considered cases fulfilled the design constraints: CBC < 2,000 ppm, and a negative MTC. The DC value for all cases is negative and varies in a relatively limited range -1.46 to -1.68 pcm/˚C. Considerable reactivity penalty related to poor burnup characteristics of Hf and Er seems unavoidable.

Table II-2: Summary of Results for Potentially Feasible BP Designs

Case Designation	CBC BOC, ppm	Cycle penalty, EFPD	DC, pcm/˚C	MTC, pcm/˚C
			BOL	BOL
Homo-Hf 1.50 v/o + IFBA Er	1991	104	-1.53	-25.6
Homo-Hf 1.75 v/o + IFBA Er	1626	123	-1.59	-27.4
Homo-Er 1.50 v/o + IFBA Hf	**1951**	**84**	**-1.46**	**-24.4**
Homo-Er 1.75 v/o + IFBA Hf	1691	95	-1.51	-25.7
Homo-Er-Enriched 1.0 v/o	**1858**	**41**	**-1.44**	**-17.5**
Homo-Er-Enriched 1.5 v/o	389	94	-1.68	-19.8

Table II-3: Enriched Er Isotopic Composition

	Natural	**Enriched**
Er-162	0.14%	0.04%
Er-164	1.61%	0.42%
Er-166	33.60%	8.72%
Er-167	**22.95%**	**80.00%**
Er-168	26.80%	6.96%
Er-170	14.90%	3.87%
Total	100.00%	100.00%

Finally, the two BP designs selected for the next stage of analysis: **Homo-Er (1.50 v/o) + IFBA Hf** and **Homo-Er-Enriched (1.0 v/o).** These two cases will be investigated by carrying out full core, 3D calculations, modeling the FFF core with 3-batch, 18-month cycle.

Two outstanding items will be addressed: controllability of the core, including viability of reactivity control and achieved temperature coefficients to address safety related issues, and economic impact of reactivity penalty and utilization of enriched BP materials.

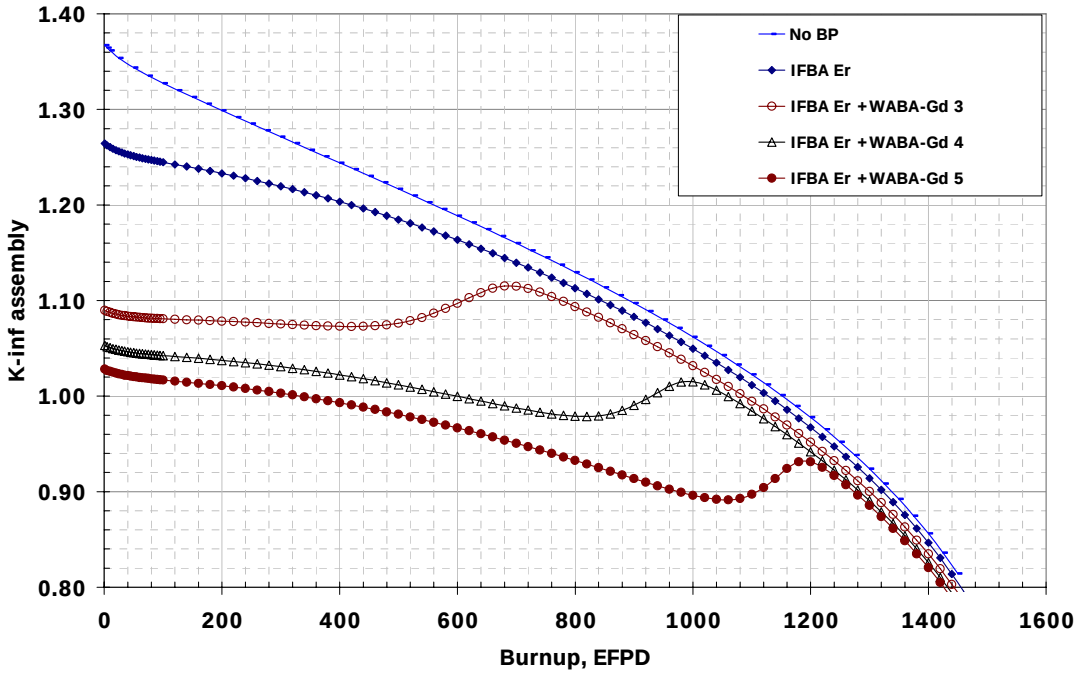

Figure II-1. Assembly Criticality for Combined WABA-IFBA BP Designs

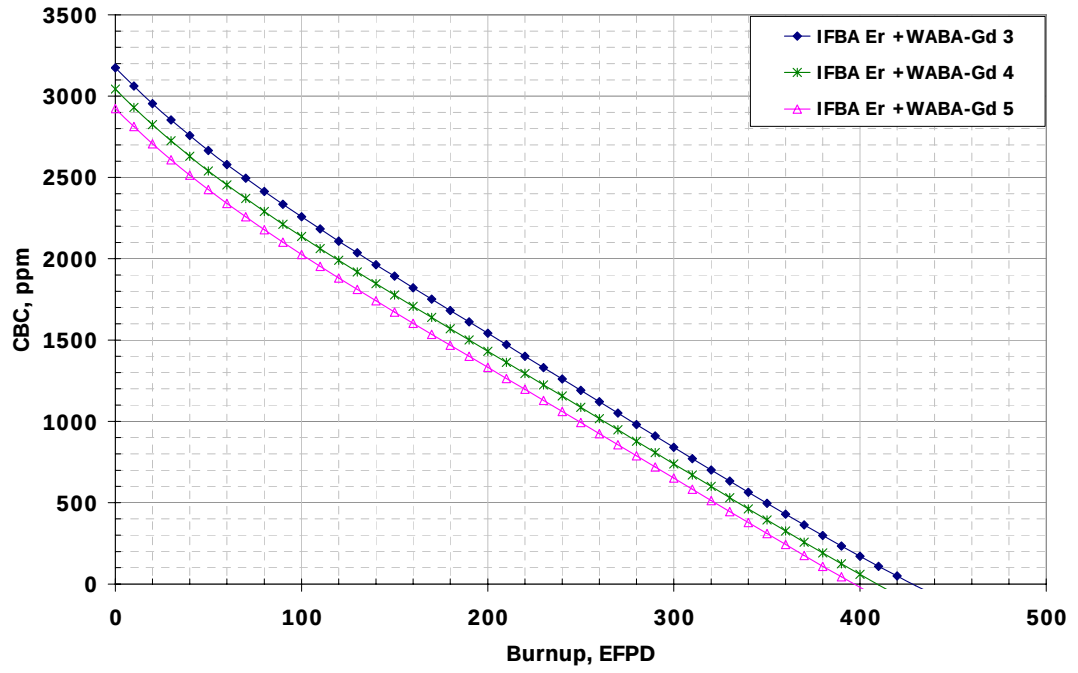

Figure II-2. Core CBC for Combined WABA-IFBA BP Designs

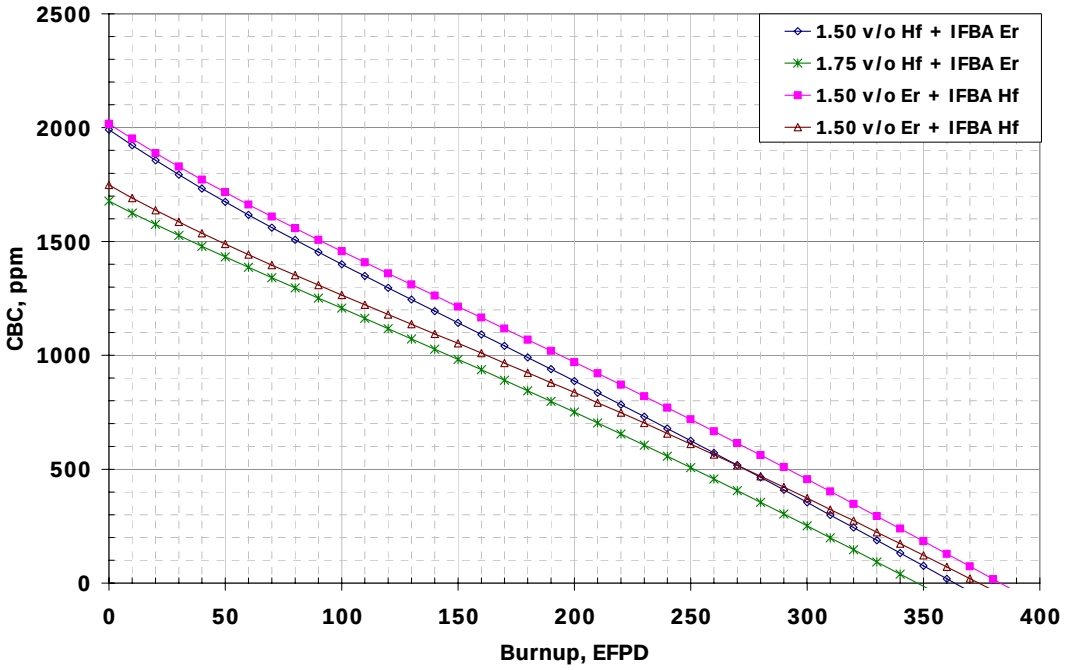

Figure II-3. Core CBC for Combined HOMO-IFBA BP Designs

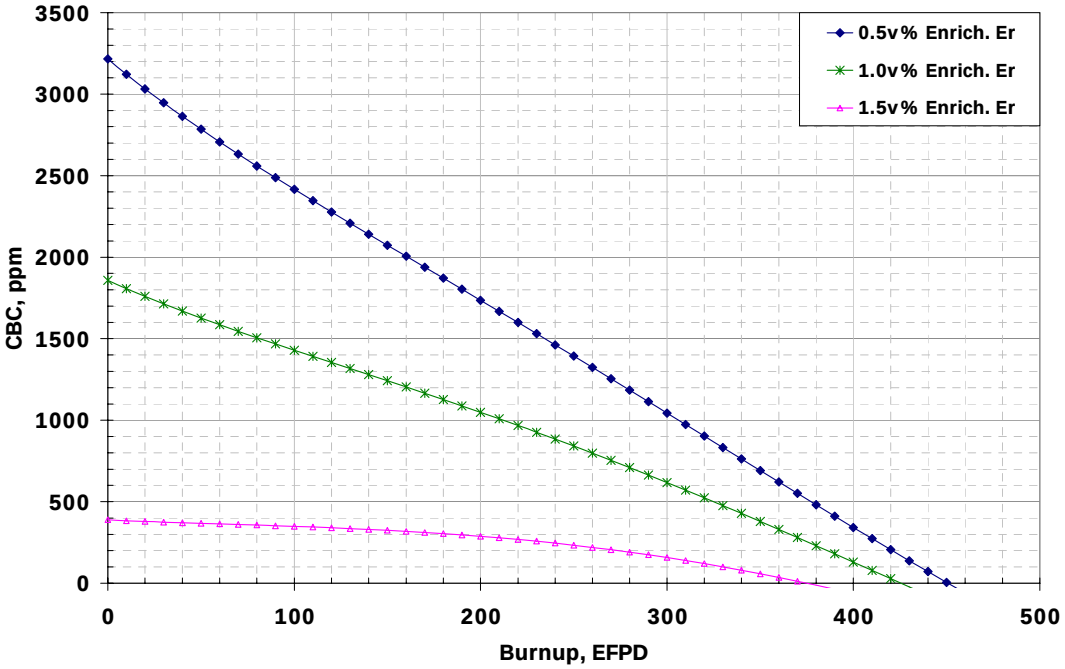

Figure II-4. Core CBC for Enriched Er HOMO BP Designs

III. Task 3: Modification of Thermal-Hydraulic Module in SILWER Code

Various fuel cycle concepts for plutonium incineration in existing PWR loaded with Inert Matrix Fuel (IMF), in which uranium is replaced by neutron-transparent inert matrix material, are currently under investigation at BGU. Some of the studied designs include ZrO_2-based IMF with annular fuel geometry and ZrO_2-MgO based IMF with the relative amount of MgO varied from 30v/o to 70v/o. These concepts are analyzed via detailed three-dimensional full core simulation of existing PWR including thermal-hydraulic feedback. The whole core simulations are carried out with the SILWER code. The SILWER code, which is a part of the ELCOS[1] system, performs three-dimensional neutronic calculations with thermal-hydraulic feedbacks of the full reactor core. Ability of the SILWER code to simulate the operation of a modern PWR loaded with all-UO2 fuel was demonstrated in the past[2]. However, two important limitations of the SILWER code with regards to the IMF analysis should be noted.

1. During fuel temperature calculations, SILWER thermal-hydraulic module employs the thermal conductivity of UO_2. These data cannot be applied to IMF because the thermal conductivity of IMF differ from UO2 and depends on inert matrix material composition (Figure III-1).
2. Thermal-hydraulic module performs fuel temperature calculations assuming solid fuel pellet geometry even for the annular fuel. Thus, in order to adapt the SILWER code for simulation of PWR core loaded with IMF several modifications to the SILWER code were made.

This section of the report summarizes these modifications and presents the effect of the modifications on the accuracy of calculation.

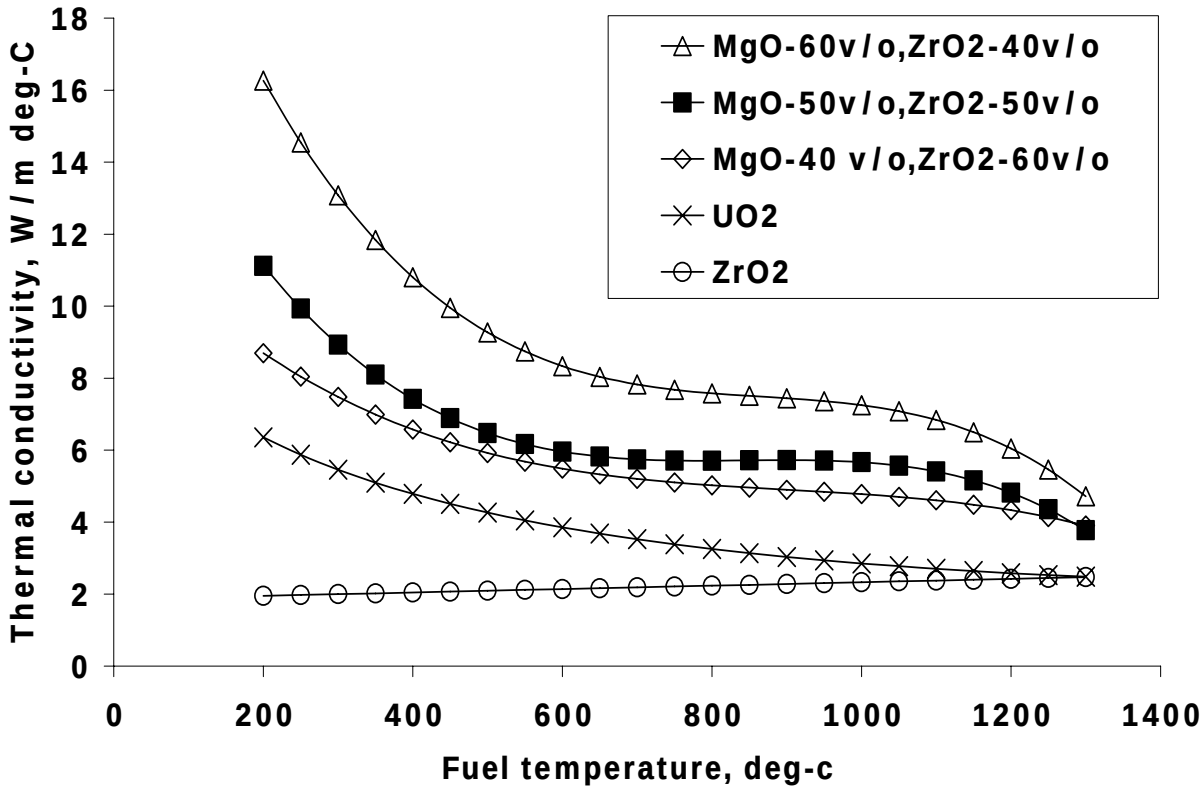

Figure III-1: Thermal conductivity of various fuel matrices[3,4].

III.1 Summary of modifications

External data file

Actual thermal conductivity data and internal radius of the annular fuel pellet are provide to the SILWER via external ASCII file called THERMC.

Fuel thermal conductivity

In modified version of SILWER, the fuel thermal conductivity as a function of temperature is given in the form of the third order polynomial (1). The polynomial coefficients are read from THERMC file.

$$k(T) = aT^3 + bT^2 + cT + d \tag{1}$$

where:

T - Fuel temperature, °C

k - Thermal conductivity of the fuel, W/m · °C

a,b,c,d - Coefficients

Temperature distribution in solid and annular fuel pellets

The temperature distribution in a solid and annular fuel pellets is given by (2) and (3) respectively[4]:

$$\int_{T}^{T_{\max}} k dT = \frac{q''' r^2}{4} \tag{2}$$

$$\int_{T}^{T_{\max}} k dT = \frac{q''' r^2}{4}\left[1 - \frac{\ln(R_{fo} / R_V)^2}{(R_{fo} / R_V)^2 - 1}\right] \tag{3}$$

where:

T - Fuel temperature, °C

k - Thermal conductivity of the fuel, W/m · °C

q''' - Volumetric heat generation rate, w/m^3

r - Distance from the center of the pellet, m

R_{fo} - Outer radius of the fuel pellet, m

R_V - Internal cavity radius of the fuel pellet, m

The equation (1) is implemented in a previous version of SILWER code by dividing the fuel pellet into the four regions (Fig. 2) with equal volume while assuming the constant thermal conductivity in each region:

$$T_{m-1} = T_m + \frac{q''' R_{fo}^{\,2}}{4 \cdot NF \cdot k_m}, \quad m = (NF + 1, NF, ..., 2, 1) \tag{4}$$

where:

T_m - Fuel temperature, °C

k_m - Thermal conductivity of the m-th radial fuel region, W/m · °C

R_{fo} - Fuel pellet radius, m

NF - Number of radial fuel zones

For an annular fuel pellet, the expression for temperature distribution was added and is given by (5). SILWER automatically chooses the proper equation depends on the inner fuel pellet radius given in THERMC file.

$$T_{m-1} = T_m + \frac{q''' R_{fo}^{\,2}}{4 \cdot NF \cdot k_m} \left[1 - \frac{\ln(R_{fo} / R_V)^2}{(R_{fo} / R_V)^2 - 1} \right] \tag{5}$$

III.2 Effect of modifications on core parameters

In this section, we explore the sensitivity of the core parameters to a) variations in fuel thermal conductivity, and b) variations in fuel rod geometry. As a study case, we consider three-dimensional model of IMF PWR core proposed and evaluated at Paul Scherrer Institute (PSI) and

reported in Ref 5. The selected core was calculated with varied fuel thermal conductivities and fuel pellet geometries. All calculations were performed with modified version of SILWER code. The list of calculated cases is presented in Table III-1.

Table III-1: List of Calculated Cases

Case	Thermal conductivity data	Fuel pellet geometry
1	ZrO2	Solid
2	UO2	Solid
3	MgO-40 v/o,ZrO2-60v/o	Solid
4	MgO-50v/o,ZrO2-50v/o	Solid
5	MgO-60v/o,ZrO2-40v/o	Solid
6	ZrO2	Annular

Table III-2 reports the sensitivity of the core parameters to the thermal conductivity of different matrix compositions. The results presented in Table III-2 demonstrate high sensitivity of the fuel temperature to variations in thermal conductivity. The difference in maximum fuel temperature for different matrix compositions can exceed 1200 °C. In addition, Table III-2 demonstrates the effect of reduction of fuel cycle length with increasing of the fuel temperature. This effect is attributed to negative Doppler coefficient of the considered fuel. The difference in discharge burnup can reach 27 EFPD.

Table III-3 presents the sensitivity of core parameters to variations in fuel pellet geometry. Taking into account the annular fuel pellet geometry results in significantly lower fuel temperature. As a consequence, the core reactivity increases due to the negative Doppler coefficient and results in higher critical boron concentration for the same thermal conductivity data.

Figure III-2 summarizes graphically the effect of the fuel matrix thermal conductivity and fuel pellet geometry on the radial temperature distribution within the fuel pellet. All cases presented in Figure III-2 are plotted for identical linear power rating.

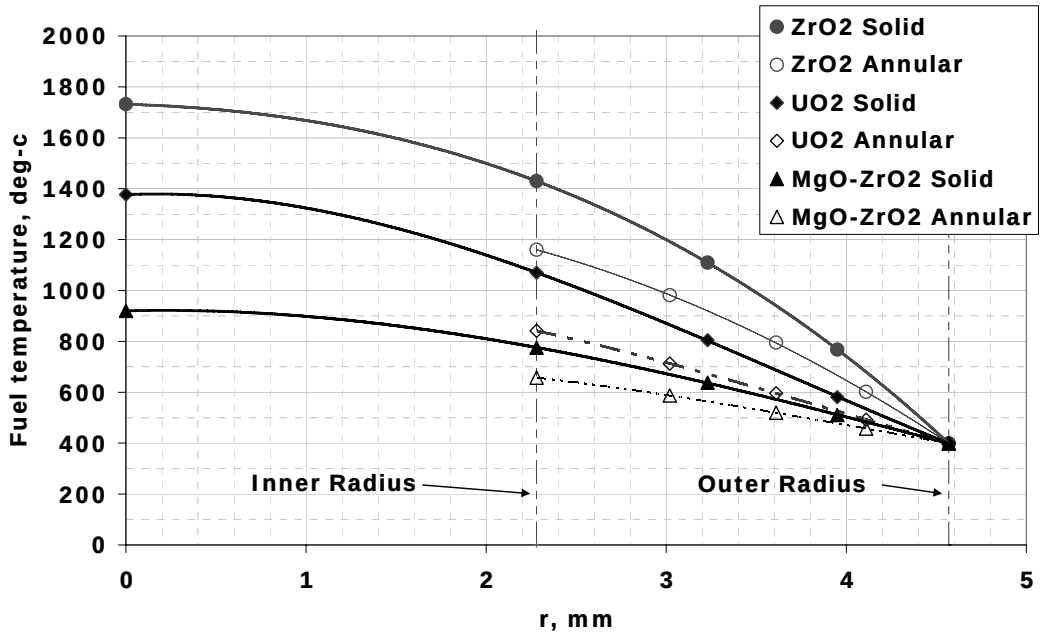

Figure III-2: Radial fuel temperature distribution for different pellet geometries and fuel matrices

In summary, the results of calculations demonstrate the importance of using the actual thermal conductivity data and fuel pellet geometry. The use of thermal conductivity data of UO_2 for different inert matrix compositions and ignoring annular fuel pellet geometry introduces significant error into calculations.

Table III-2: Sensitivity of core parameters to the thermal conductivity of matrix composition

Case	K ave BOC, W/m °C	T_{fuel} ave. BOC, °C	T_{fuel} max. BOC, °C	FC length, EFPD	Δ FC length,* EFPD
1	2.22	774	1928	338	0
2	4.06	582	1633	353	15
3	5.25	429	1154	357	18
4	6.70	496	1063	359	21
5	10.07	413	667	366	27

* Compared to ZrO_2 case

Table III-3: Sensitivity of core parameters to variations in fuel pellet geometry

Case	Fuel pellet geometry	CBC, ppm	T_{fuel} Average, °C	T_{fuel} Max., °C	DC, pcm/°C
1	Solid	1382	774	1928	-1.5
6	Annular	1461	592	1300	-1.8

IV. Task 4: Performance Characteristics of Fully Fertile Free PWR Core

This section of the report presents the results of 3-dimensional whole core analysis of PWR fully loaded with fertile free fuel. Based on the preliminary assembly level calculations, three most promising combinations of BP designs were selected for the full core 3D simulation:

- Hf Homogeneously mixed with fuel – Er IFBA coating – Boron WABA
- Er Homogeneously mixed with fuel – Hf IFBA coating – Boron WABA
- Enriched Er Homogeneously mixed with fuel

The following core characteristics were addressed in this task:

- Core loading and cycles length
- Critical soluble boron concentration
- Power peaking factors
- Materials flow
- Distributed Doppler Coefficient
- Uniform Doppler Coefficient
- Moderator Temperature Coefficient
- Soluble Boron Reactivity Worth
- Fuel temperature distribution

The objective of the current task is to compare several FFF core options with previously reported design and with a standard UO_2 fuel PWR core. Similarity of the FFF core performance parameters to those of the conventional fuel PWR core will indicate potential feasibility of the fertile free fuel utilization in PWRs.

IV.1 Analysis Methodology and Reference Core Description

The calculations were performed with 3-dimensional nodal diffusion code SILWER. The code is a part of the ELCOS [1] LWR analysis software package. The SILVER code includes thermal hydraulic feedback to the neutronic module. The thermal module of the code calculates fuel and

moderator temperature distributions, distribution of coolant flow and pressure drop in individual assembly channels and a set of additional thermal hydraulic parameters. The code does not account for the coolant cross-flow (communication) between the channels. The original SILWER module responsible for the calculation of fuel temperature distribution was modified to allow analysis of non-UO_2 fuels and annular fuel pellets. The description of the performed modifications and verification of the modified module results are presented in the 3rd progress report of the current project [2].

The analysis was performed for a standard Westinghouse PWR core loaded with 193 of 17×17 fuel rods fuel assemblies. Major core design and operating parameters assumed in this analysis are summarized in Table IV-1.

The fuel designs evaluated in this task are summarized in Table IV-2. Cases 1, 2, and 3 represent previously chosen most promising fertile free fuel designs Homogeneously mixed Hf-IFBA Er, Homogeneously mixed Er-IFBA Hf, and Homogeneously mixed enriched Er respectively. Cases 4 and 5 correspond to the PSI FFF core design and standard UO_2 fuel respectively.

The enriched Er isotopic composition used in Case 3 is presented in Table IV-3. The Plutonium isotopics used for the analysis corresponds to that found in a typical LWR spent fuel with 4.2% initial enrichment, 50 MWd/kg discharge burnup, after 10 years of decay. The Pu isotopic composition is presented in Table IV-4.

The fuel assemblies are reloaded in 3 equal batches with approximately 18 calendar months fuel cycle. The fuel loading map for the Cases 1, 2, and 3 is presented in Figure IV-1.

In addition to the three fertile free fuel designs chosen for the analysis, the results of the reference standard all-UO_2 fuel as well as previously reported fully FFF core design developed at PSI [3] are included in this report for the comparison purposes. Note that the PSI design is developed for a smaller PWR core with the 4-batch fuel management and annual fuel cycle. Additional details on PSI design can be found in References 3 and 4.

For each fuel design option, equilibrium core was approximated through a number of sucessive fuel reloads starting with initial guess of burnup distribution for the once and twice burned fuel batches. Such itterative process was repeated untill the average initial burnup of batch *n* was equal to the discharge burnup of batch *n-1* in the same cycle, where *n = 1,2,3* for the fresh, once, and twice burned fuel batch respectively.

Table IV-1: Parameters of the reference PWR core

Operating parameter	**Value**
Core	
Total thermal output (MWth)	3358
Number of fuel assemblies in the core	193
Average core power density (MW/MTHM)	37.3
System pressure (bar)	155
Total core flow rate (kg/s)	18600
Core inlet temperature (ºC)	289.1
Fuel Assembly	
Active fuel height (cm)	366
Assembly array	square 17 × 17 rods
Total number of fuel rods per assembly	264
Number of grids per assembly	7
Assembly pitch (cm)	21.5
Assembly gap (cm)	0.08
Fuel rod pitch, cm	1.26
Number of guide tubes	25
Guide tube inner radius (cm)	0.5715
Guide tube outer radius (cm)	0.6120
Fuel Rod	
Cladding outer radius (cm)	0.4750
Cladding thickness (cm)	0.0570
Cladding material	Zircaloy
Fuel pellet radius (cm)	0.4095

Table IV-2: Analyzed Fuel Designs Description

Analyzed Case	***1***	***2***	***3***	***4***	***5***
Fuel matrix composition, MgO/ZrO_2 (vol.%)	50/50	50/50	50/50	0/100	UO_2
Pu content (vol. %)	10.3	10.3	8.0		4.21(*)
Homogeneously mixed BP material	HfO_2	Er_2O_3	Enriched Er_2O_3	Er_2O_3	-
Homogeneously mixed BP content (vol. %)	1.5	1.5	1.0	5.4	-
IFBA Coating Material	Er_2O_3	HfO_2	-	-	ZrB_2
IFBA Coating Thickness, mm	0.0160	0.0160	-	-	0.0115
Number of IFBA rods in assembly	264	264	-	-	116
WABA burnable absorber	Al_2O_3 - B_4C		-	-	Al_2O_3 - B_4C
Number of WABA rods in assembly	24		-	-	4 - 16
B-10 loading (g/cm of WABA rod)	0.006165		-	-	0.006165

(*) Max. Uranium enrichment in All-UO_2 fuel case

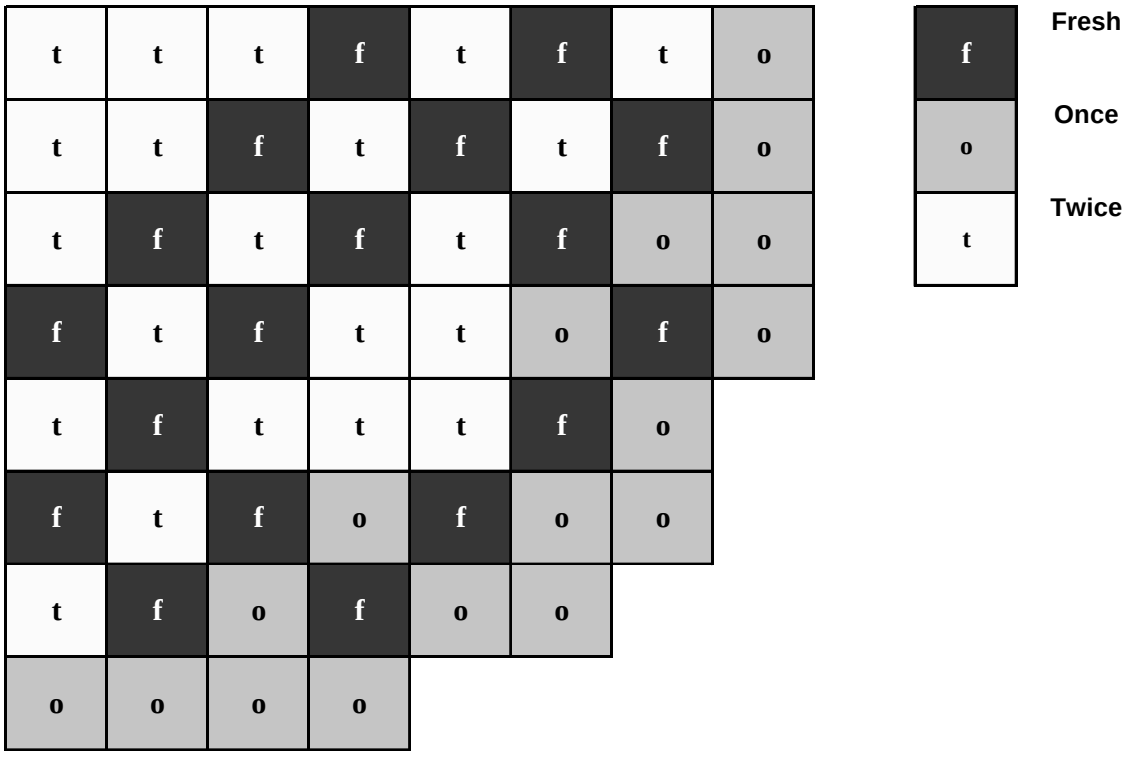

Figure IV-1: Loading pattern for Cases 1-3

Table IV-3: Enriched Er Isotopic Composition

Isotope	*wt. %*
Er162	0.04
Er164	0.41
Er166	8.67
Er167	79.96
Er168	6.99
Er170	3.94

Table IV-4: Plutonium Isotopic Composition

Isotope	*wt. %*
Pu238	3.2
Pu239	56.3
Pu240	26.6
Pu241	8.0
Pu242	5.8

IV.2 Results and Discussion

Core loading and cycle length

The objectives of nuclear design of a PWR core are to achieve the desired fuel cycle length of 18-month while maintaining all safety parameters of the core within the safety envelope and ensuring criticality control. Fertile free cores have additional objective of maximizing the fraction of Pu burned during the reactor campaign.

The fissile loading of the fuel was adjusted to achieve fuel cycle length of 470 EFPD ±5 % (equivalent to 18 calendar months) assuming 3 batch refueling scheme. The amount of burnable poison was varied to reduce the soluble boron concentration below 2000 ppm as mandated by the reactor safety and operational requirements. For the FFF designs (Case 1 and 2), all fuel rods in the assembly had IFBA coating, therefore the adjustment of burnable poison loading was realized

through variation of volume fraction of the BP homogeneously mixed with the fuel. The effect of such Pu and BP loading adjustments on fuel cycle length and maximum soluble boron concentration was estimated on the basis of 2-dimentional fuel assembly Non-Linear Reactivity Model analyses performed in the Year-1 of the current project. The estimates based on the 2D analyses results showed excellent accuracy once verified and compared with the detailed full core simulation results. Thus, Non-Linear Reactivity Model proved to be extremely valuable tool for PWR core design, in particular, for fertile free fuel analyses.

The calculations performed in this Task showed that the reduction in fuel cycle length for FFF designs due to the incomplete depletion of burnable poison (cycle penalty) can be significantly reduced if some part of the BP material homogeneously mixed with the fuel is replaced with standard WABA burnable absorbers. As a result, the final FFF burnable poison designs included WABAs in addition to Er/Hf homogeneously mixed with the fuel and as IFBA coating (Table IV-2).

Figure IV-2 presents the critical boron concentration (CBC) letdown curves as calculated by the SILWER code for 3-dimensional PWR core model and all considered cases. All considered fuel options can achieve their target cycle length with maximum critical boron concentration below 2000 ppm.

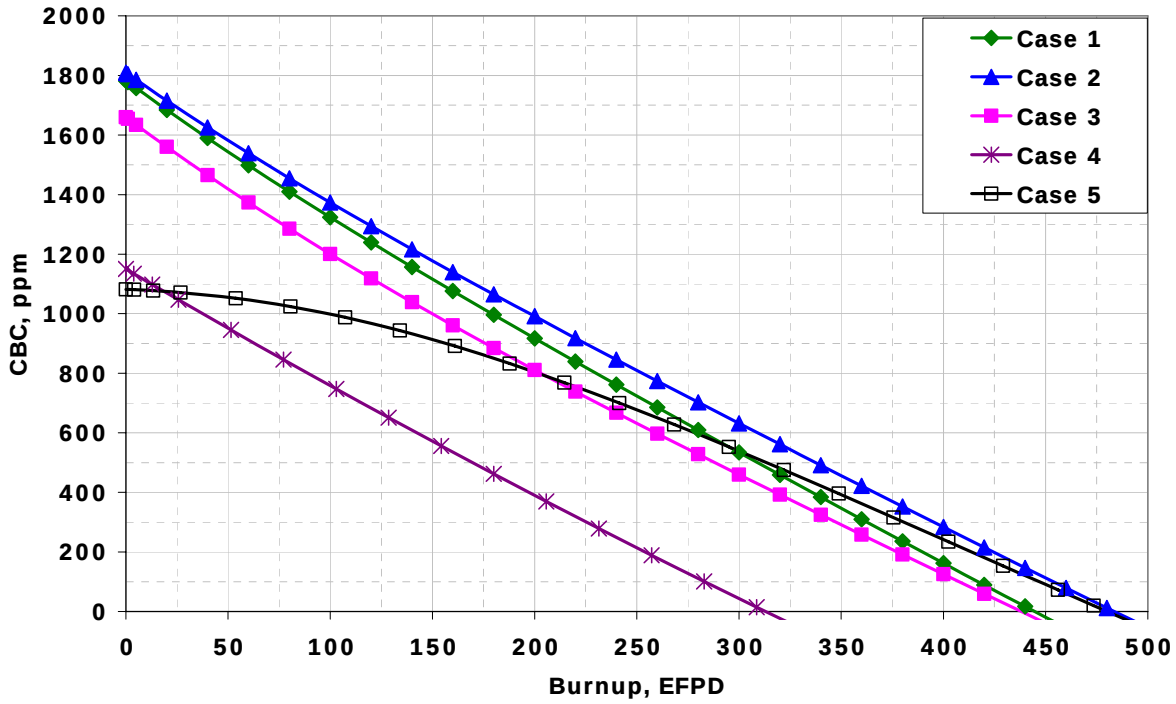

Figure IV-2: CBC Letdown Curves

Table IV-5 summarizes the most important core performance characteristics of all calculated cases. Among the analyzed FFF cases, the enriched Er case is slightly more advantageous to other cases since it requires the lowest Pu loading to achieve the required cycle length. However, this advantage will most certainly not offset the considerable costs associated with Er enrichment [5]. Detailed economic evaluation of the fuel cycle based on fertile free fuel would be required to explore systematically the justification of using enriched burnable poisons. Such analysis is beyond the scope of the current project.

For the same reason of lower Pu loading for required cycle length, Er-Hom/Hf-IFBA (Case 2) option is somewhat more preferable to the Hf-Hom/Er-IFBA (Case 1) option. Moreover, the discharge burnup is the highest and therefore the Pu destruction is most efficient for the Case 3, then for Case 2. Case 1 exhibits the lowest discharge burnup and the lowest burned Pu fraction. Since all fertile free fuels would burn the same mass of Pu per unit energy produced by the fuel, the only difference between different designs is the efficiency of Pu destruction. The higher the efficiency of Pu destruction, the lower would be Pu inventory in the core. Low Pu loading cores

are very beneficial from the core design perspective because nearly all FFF-Pu core design challenges aggravate with an increase in Pu loading.

The power peaking factors are within acceptable limits for all considered cases, which indicate potential feasibility of thermal hydraulic performance of the analyzed cores. Although no specific effort was made in this study to optimize the fuel loading pattern of analyzed cases to achieve the lowest power peaking factors, the conventional all-UO_2 core seems to be less restrictive with regards to the power peaking therefore loading pattern choice.

Detailed maps of the core radial power distribution for Cases 1, 2, and 3 are presented in Figures IV-3 through IV-5 respectively. The discharge burnup distribution maps for Cases 1, 2, and 3 are presented in Figures IV-6 through IV-8 respectively.

The efficiency of individual Pu isotopes destruction in each analyzed case is summarized in Table IV-6. In the Enriched Er case over 65% of initial Pu can be destroyed per pass through the reactor. The destroyed Pu fraction for the Hf-Hom/Er-IFBA (Case 1) and Er-Hom/Hf-IFBA (Case 2) options are close to 55%.

As can be observed from Table IV-6, the proliferation resistance of the Pu isotopic composition in the discharged fertile free fuel is greatly enhanced for all considered options with some advantage of the Enriched Er case. Pu239 content is reduced from 56% to about 20% for the Case 1 and to about 9% for the Case 3. The fraction of “even” Pu isotopes with high spontaneous fission source is increased by about a factor of 2 in all cases. The fraction of Pu238 with high heat emission is also increased from 3.2% to about 5% in all cases.

Table IV-5: Summary of the Core and Fuel Cycle Performance Characteristics

	Case 1		Case 2		Case 3		Case 4 (PSI)		Case 5 (UO2)	
Initial Pu loading, kg/assy	49.8		49.8		38.7		43.4		-	
Fuel Cycle Length, EFPD	447		480		438		306		465	
Aver. disch. burnup, MWd/kg	488.9		516.1		595.2		502.6		40.4	
Max. disch. burnup, MWd/kg	493.1		519.7		600.5		512.4		46.9	
	BOC	**EOC**	**BOC**	**BOC**	**BOC**	**BOC**	**BOC**	**EOC**	**BOC**	**EOC**
Radial Peak	1.45	1.33	1.43	1.35	1.47	1.47	1.43	1.38	1.28	1.32
Nodal Peak	1.87	1.60	1.83	1.64	1.93	1.84	1.86	1.69	1.56	1.54

Table IV-6: BOL and EOL Concentrations of Pu and Minor Actinides

(kg/assembly)

	Case 1		Case 2		Case 3		Case 4 (PSI)		Case 5 (UO2)	
	BOC	**EOC**	**BOC**	**EOC**	**BOC**	**EOC**	**BOC**	**EOC**	**BOC**	**EOC**
Pu238	1.6	1.1	1.6	1.1	1.2	0.7	1.2	0.9	0.0	0.2
Pu239	28.1	4.7	28.1	3.6	21.8	1.1	23.6	2.9	0.0	3.0
Pu240	13.3	9.3	13.3	8.6	10.3	5.0	9.9	6.6	0.0	1.5
Pu241	4.0	5.0	4.0	4.7	3.1	2.8	5.1	3.8	0.0	0.9
Pu242	2.9	3.8	2.9	3.9	2.3	3.5	3.6	4.5	0.0	0.5
Total Pu	**49.8**	**23.9**	**49.8**	**21.9**	**38.7**	**13.3**	**43.4**	**18.6**	**0.0**	**6.2**
ΔPu, EOC-BOC		-26.0		-27.9		-25.4		-24.8		6.2
Am241	0.00	0.38	0.00	0.36	0.00	0.18	0.00	0.30	0.00	0.03
Am243	0.00	0.95	0.00	1.00	0.00	0.90	0.00	1.02	0.00	0.00
Cm242	0.00	0.10	0.00	0.11	0.00	0.10	0.00	0.10	0.00	0.01
Cm244	0.00	0.65	0.00	0.74	0.00	0.69	0.00	0.69	0.00	0.06
Cm245	0.00	0.05	0.00	0.07	0.00	0.07	0.00	0.08	0.00	0.00
Tot. MA	**0.00**	**2.14**	**0.00**	**2.29**	**0.00**	**1.94**	**0.00**	**2.19**	**0.00**	**0.11**

1.32 0.82	1.33 0.87	1.33 0.97	1.43 1.31	1.22 1.06	1.19 1.31	0.87 0.94	0.57 0.73
1.33 0.87	1.33 0.91	***1.45*** 1.25	1.29 1.03	1.33 ***1.33***	1.08 1.05	0.96 1.17	0.57 0.74
1.33 0.97	***1.45*** 1.25	1.30 1.01	1.38 1.28	1.18 1.02	1.17 1.29	0.94 1.06	0.54 0.71
1.43 1.31	1.29 1.03	1.38 1.28	1.20 0.97	1.13 0.97	1.09 1.11	0.81 1.03	0.40 0.58
1.22 1.06	1.33 ***1.33***	1.18 1.02	1.13 0.97	1.01 0.94	0.92 1.11	0.60 0.79	
1.19 1.31	1.08 1.05	1.17 1.29	1.09 1.11	0.92 1.11	0.70 0.87	0.38 0.55	
0.87 0.94	0.96 1.17	0.94 1.06	0.81 1.03	0.60 0.79	0.38 0.55		
0.57 0.73	0.57 0.74	0.54 0.71	0.40 0.58				

Key:

Assembly relative power at:

0.780 **BOC**
0.855 **EOC**

Max. relative power at:

1.45 **BOC**

1.33 **EOC**

Figure IV-3: Case 1 - Radial Power Distribution Map

1.29 0.81	1.30 0.86	1.30 0.96	1.41 1.34	1.21 1.06	1.19 1.33	0.87 0.93	0.58 0.73
1.30 0.86	1.30 0.90	***1.43*** 1.26	1.27 1.03	1.33 ***1.35***	1.08 1.04	0.97 1.18	0.58 0.73
1.30 0.96	***1.43*** 1.26	1.28 1.00	1.37 1.29	1.17 1.01	1.18 1.31	0.96 1.07	0.55 0.71
1.41 1.34	1.27 1.03	1.37 1.29	1.18 0.96	1.12 0.95	1.11 1.11	0.82 1.04	0.41 0.57
1.21 1.06	1.33 ***1.35***	1.17 1.01	1.12 0.95	1.01 0.93	0.94 1.12	0.62 0.79	
1.19 1.33	1.08 1.04	1.18 1.31	1.11 1.11	0.94 1.12	0.72 0.87	0.39 0.54	
0.87 0.93	0.97 1.18	0.96 1.07	0.82 1.04	0.62 0.79	0.39 0.54		
0.58 0.73	0.58 0.73	0.55 0.71	0.41 0.57				

Key:

Assembly relative power at:

0.780 **BOC**
0.855 **EOC**

Max. relative power at:

1.43 **BOC**

1.35 **EOC**

Figure IV-4: Case 2 - Radial Power Distribution Map

1.43 0.83	1.25 0.68	1.24 0.69	1.23 0.73	1.36 0.96	1.13 0.87	1.10 1.41	0.60 0.89
1.25 0.68	***1.47*** 0.98	1.22 0.69	1.45 1.10	1.19 0.80	1.24 1.10	1.07 1.42	0.58 0.88
1.24 0.69	1.22 0.69	1.21 0.71	1.19 0.76	1.38 1.29	1.05 0.93	1.00 1.43	0.52 0.85
1.23 0.73	1.45 1.10	1.19 0.76	1.29 0.97	1.08 0.87	1.14 ***1.47***	0.84 1.33	0.39 0.71
1.36 0.96	1.19 0.80	1.38 1.29	1.08 0.87	0.97 0.92	0.96 1.41	0.58 0.94	
1.13 0.87	1.24 1.10	1.05 0.93	1.14 ***1.47***	0.96 1.41	0.66 1.00	0.35 0.65	
1.10 1.41	1.07 1.42	1.00 1.43	0.84 1.33	0.58 0.94	0.35 0.65		
0.60 0.89	0.58 0.88	0.52 0.85	0.39 0.71				

Key:

Assembly relative power at:

0.780 **BOC**
0.855 **EOC**

Max. relative power at:

1.47 **BOC**

1.47 **EOC**

Figure IV-5: Case 3 - Radial Power Distribution Map

468400	474700	485300	221300	489300	205100	452800	300700
474700	478900	215600	***490400***	217200	478200	174100	300500
485300	215600	488600	215000	482300	201700	358800	295800
221300	***490400***	215000	478400	473400	374300	149500	272900
489300	217200	482300	473400	462100	165600	307000	
205100	478200	201700	374300	165600	321900	268500	
452800	174100	358800	149500	307000	268500		
300700	300500	295800	272900				

Max. Discharge Burnup

490400

Figure IV-6: Case 1 - Discharge Burnup (MWd/t) Distribution Map

492500	499900	512600	237600	***519800***	224000	484700	315700
499900	505000	229800	519700	235200	510300	193500	315900
512600	229800	517100	230900	512800	222400	380500	311500
237600	519700	230900	507200	503700	395700	168600	286000
519800	235200	512800	503700	493400	185100	324100	
224000	510300	222400	395700	185100	340600	281100	
484700	193500	380500	168600	324100	281100		
315700	315900	311500	286000				

Max. Discharge Burnup

519800

Figure IV-7: Case 2 - Discharge Burnup (MWd/t) Distribution Map

558800	568500	584800	273600	***596000***	262000	561200	381500
568500	575000	260900	594200	273000	587400	224600	381800
584800	260900	590600	264100	587400	257500	453100	377100
273600	594200	264100	579700	576800	468100	195000	350600
596000	273000	587400	576800	566900	211900	391500	
262000	587400	257500	468100	211900	407700	343700	
561200	224600	453100	195000	391500	343700		
381500	381800	377100	350600				

Max. Discharge Burnup

596000

Figure IV-8: Case 3 - Discharge Burnup (MWd/t) Distribution Map

IV.3 Evaluation of Reactivity Coefficients

This section presents the results of the reactivity coefficients calculations, soluble boron reactivity worth and fuel temperature distribution in the reactor core.

The reactivity coefficients were calculated for the Hot Full Power (HFP), equilibrium Xe, and All Rods Out (ARO) core operating conditions.

The Distributed Doppler Coefficient (DDC) was calculated as the reactivity change associated with a change in fuel temperature with the same spatial distribution as the power divided by the change in the averaged fuel temperature. Namely, the change in the average fuel temperature due to a given change in power is consistent with a new power distribution. This reactivity coefficient is considered a conservative estimate of the Doppler Effect in evaluation of accidents which result in unintentional cooling down events, such as Loss of Heat Sink (LOHS) resulting from main steam line break.

The Uniform Doppler Coefficient (UDC) was calculated as the reactivity change associated with a uniform change in the fuel temperature divided by the change in the averaged fuel temperature. In the UDC calculation, the fuel temperature is assumed to be constant over the whole core and is changed uniformly conserving all other core parameters and distributions. As oppose to DDC, the UDC tends to underestimate the magnitude of the Doppler effect. Therefore, the UDC value is conservative if used for evaluation of reactivity initiated accidents (e.g. control rod ejection) in which negative reactivity feedback is beneficial.

Moderator Temperature Coefficient (MTC) of a PWR core was calculated as the reactivity change associated with a change in coolant inlet temperature divided by the change in the core average coolant temperature.

Finally, Soluble Boron Reactivity Worth (BW) was calculated as the change in the core reactivity as a result in the change in Soluble Boron concentration in the reactor coolant divided by the core average Soluble Boron concentration.

The summary of the calculated reactivity coefficients in all considered cases is presented in Table IV-7. The reactivity coefficients are negative at all time points during the cycle for all calculated cores. All fertile free cores exhibit approximately the same negative Doppler feedback, which is determined primarily by the type and the loading of the burnable poison in use. Homogeneously mixed Hf case (Case 1) shows the most negative Doppler coefficient. The magnitude of the Doppler feedback is still somewhat lower than that of the reference UO_2 fuel core (-1.8 -1.5 pcm/°C for the FFF cores versus 3.0 pcm/°C for the UO_2 core). The assessment of the importance and consequences of such a difference is beyond the scope of the current project. Such analysis would require a detailed evaluation of the selected accidents condition where the Doppler Effect plays an important role (e.g. control rod ejection accident). The very fact that all FFF cores can be designed with the negative and substantial in magnitude Doppler coefficient indicates potential feasibility of such cores.

The Doppler coefficients of the FFF cores tend to decrease with the burnup and become the most restrictive (least negative) at the End of Cycle (EOC). Therefore, the UDC and DDC dependence on the core average fuel temperature was analyzed at the EOC time point. The results are presented in Figures IV-9 and IV-10. The Doppler coefficients of the FFF cores exhibit relatively week dependence on the fuel temperature decreasing by about 0.5 pcm/°C every 100°C for DDC and 0.5 pcm/°C every 400°C for UDC. The slope of these DC vs. temperature curves is about the same in all cases including UO_2 fuel. The enriched Er fuel (Case 3) exhibits the weakest dependence of DC on the fuel temperature among the considered FFF cases.

Table IV-7: Summary of feedback parameters

	Case 1		**Case 2**		**Case 3**		**Case 4 (PSI)**		**Case 5 (UO2)**	
	BOC	**EOC**	**BOC**	**EOC**	**BOC**	**EOC**	**BOC**	**EOC**	**BOC**	**EOC**
DDC, pcm/C †	-1.8	-1.6	-1.7	-1.5	-1.5	-1.5	-1.6	-1.4	-3.0	-3.3
UDC, pcm/C †	-1.5	-1.5	-1.4	-1.4	-1.2	-1.2	-1.3	-1.2	-2.7	-3.0
MTC, pcm/C *	-28.6	-57.7	-27.3	-56.6	-22.4	-54.5	-38.4	-64.2	-33.1	-68.8
BW, pcm/ppm	-2.7	-3.7	-2.7	-3.8	-3.8	-5.8	-3.4	-4.4	-7.1	-8.1

† Average fuel temperature = 650 °C

* Coolant average temperature = 300 °C

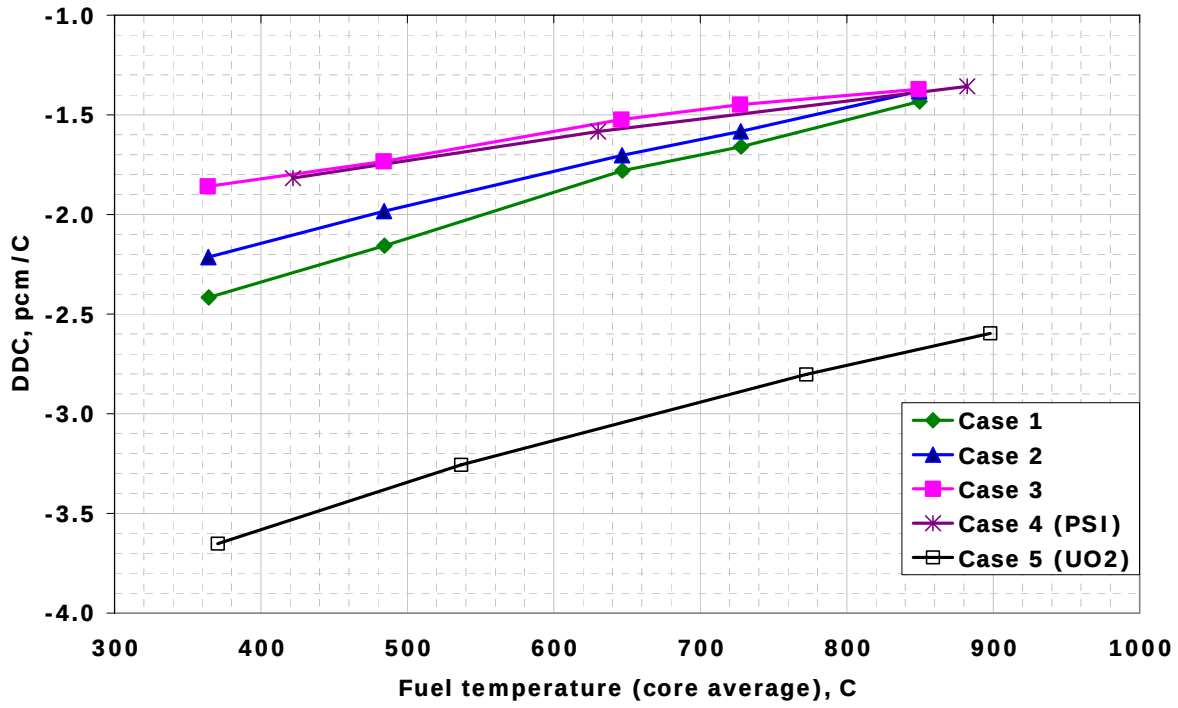

Figure IV-9: Distributed Doppler Coefficient at EOC

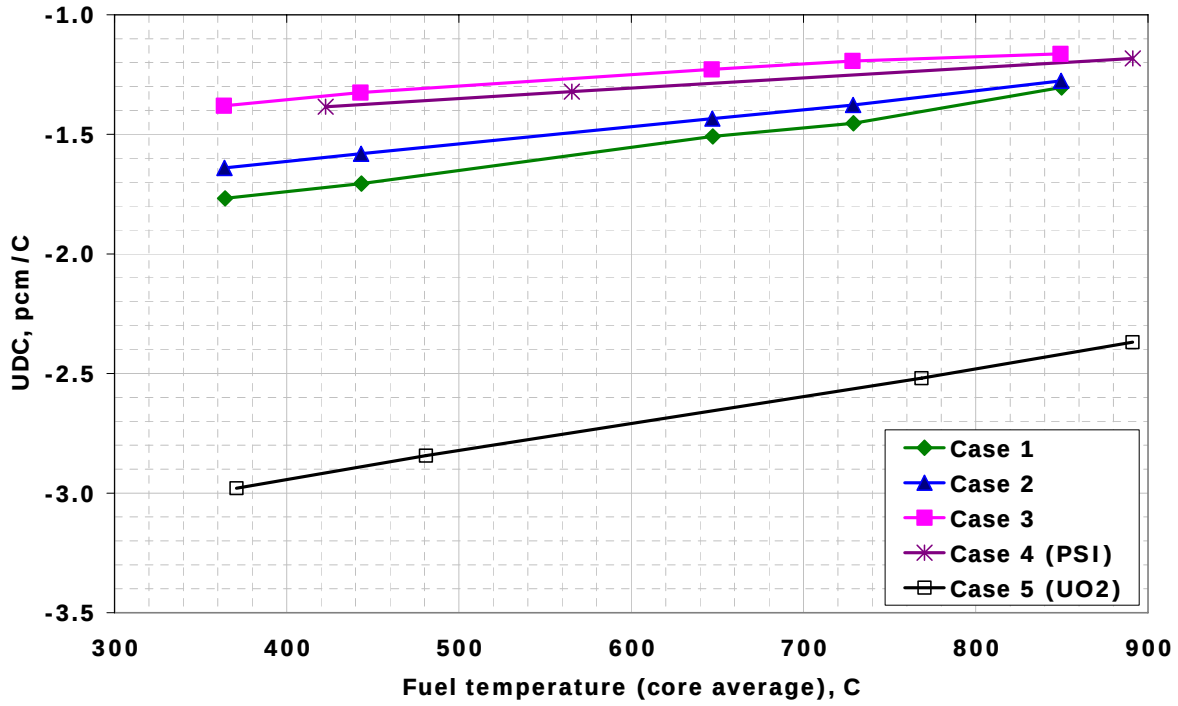

Figure IV-10: Uniform Doppler Coefficient at EOC

The calculated MTC values in all considered cases are also summarized in Table IV-7. The dependence of the MTC on the core average moderator temperature at BOC and EOC is shown in

Figures IV-11 and IV-12 respectively. Similarly to Doppler coefficients, the MTC values for all calculated FFF cores are negative and very close to those of the reference UO_2 core. At the EOC, the MTC values for all considered cores are practically identical. At the BOC, the enriched Er fuel (Case 3) exhibits the least negative MTC value, while MTC for the Case 1 and Case 2 are nearly identical and slightly more negative (by 5 to 10 pcm/°C) than the Case 3 value.

The MTC becomes more negative with the increase in moderator temperature in all cases. The rate of this MTC change is practically the same for all considered cores.

The calculated soluble Boron reactivity worth at BOC and EOC is reported in Table IV-7. As expected and predicted by the 2-dimnsional calculations, the BW of fertile free cores is lower by about a factor of two than that of the conventional UO_2 core. However, careful burnable poison design enabled the steady state reactivity control of fully fertile cores with acceptable soluble boron concentrations.

The lower than for UO_2 reactivity worth of the control materials, however, may represent a potential problem for fully fertile free cores with respect to shutdown margin requirements. The control rods must provide a sufficient shutdown margin for the FFF core at all possible conditions from Cold Zero Power, no Xe to Hot Full Power, equilibrium Xe. The existing control rod design may not be adequate to meet these requirements. A number of practical solutions are possible. The latest PWR designs include extra vessel head penetrations to allow insertion of additional control rod banks. Such reactors were designed keeping in mind possibility of the full MOX cores, which, similarly to FFF, also have low control rod worth. For older PWRs, the possible solution could be the use of control rods with Boron enriched in B-10 isotope. The enriched boron is already widely used by the nuclear industry.

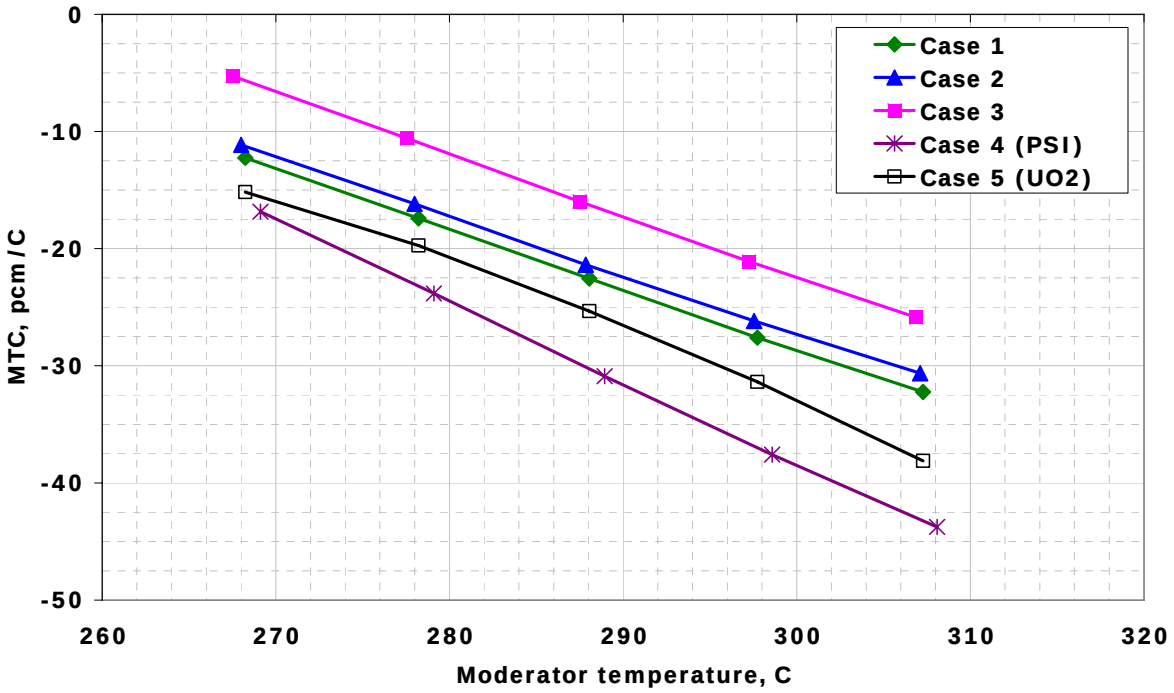

Figure IV-11: MTC vs. average moderator temperature at BOC, CBC

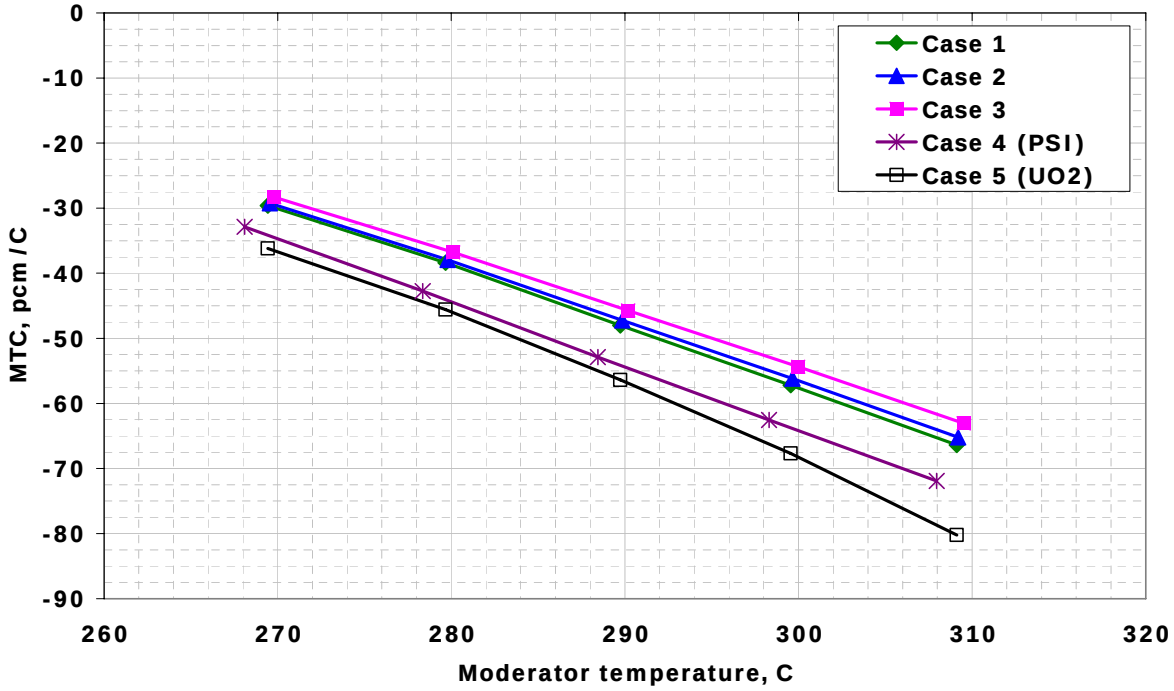

Figure IV-12: MTC vs. average moderator temperature at EOC, CBC

In addition to reactivity coefficients, the fuel temperature distributions were also calculated. The selected results are reported in Figures IV-13 – IV-21.

Figures IV-13 – IV-15 present the radial distributions of assembly average fuel temperature for the Cases 1 through 3 respectively. In general, the assembly average fuel temperature follows the core power distribution reported in progress report on the Task 4 of this project. Therefore, Case 3 (enriched Er) having the highest radial power peak also exhibit the highest assembly average fuel temperature among the FFF cores.

The assembly average fuel temperature in all FFF cores does not exceed 850°C. The core average fuel temperature in FFF cores is lower than that of the UO_2 core by about 100°C due to the better thermal conductivity of MgO-ZrO_2 fuel matrix as compared with UO_2. This advantage, however, cannot be judged on the absolute scale for two reasons. Firstly, the melting point of the MgO-ZrO_2 matrix is somewhat lower than that of the UO_2 which means that the margin to melting may even be reduced rather than improved. Secondly, the fuel melting is only represents a problem under accident conditions. Therefore, the fuel temperature at the steady state reactor operation is only one parameter in a large spectrum of the fuel thermal, nuclear, and mechanical characteristics that affect the reactor behavior in accidents.

Figures IV-16 – IV-21 present the axial core average and hot assembly fuel temperature distributions at BOC and EOC for the Cases 1 through 3 respectively. All Fertile Free cores have similar fuel temperature profiles with maximum fuel temperature in the hot assembly below 1000°C. Generally, the maximum fuel temperature in the hot assembly at EOC is lower than that at the BOC by about 100°C due to the lower axial power peaking at EOC.

761 580	766 598	765 633	800 760	728 667	716 761	599 627	492 553
766 598	765 613	***808*** 735	751 657	766 ***767***	678 663	631 710	491 554
765 633	***808*** 735	756 648	782 747	713 652	709 754	626 671	480 544
800 760	751 657	782 747	718 634	693 634	682 687	577 662	431 499
728 667	766 ***767***	713 652	693 634	650 627	620 692	504 576	
716 761	678 663	709 754	682 687	620 692	539 604	423 489	
599 627	631 710	626 671	577 662	504 576	423 489		
492 553	491 554	480 544	431 499				

Max. Fuel Tempr. at:

BOC	***808***
EOC	***767***

Figure IV-13: Case 1 - BOC and EOC average fuel temperature map (°C).

750 575	755 595	755 632	794 769	722 666	716 768	599 623	495 550
755 595	754 610	***801*** 742	744 656	764 ***776***	675 660	635 715	494 551
755 632	***801*** 742	748 647	778 754	709 648	712 760	632 671	485 542
794 769	744 656	778 754	713 630	691 628	687 687	582 665	435 495
722 666	764 ***776***	709 648	691 628	650 620	625 693	509 573	
716 768	675 660	712 760	687 687	625 693	545 602	427 484	
599 623	635 715	632 671	582 665	509 573	427 484		
495 550	494 551	485 542	435 495				

Max. Fuel Tempr. at:

BOC	***801***
EOC	***776***

Figure IV-14: Case 2 - BOC and EOC average fuel temperature map (°C).

731 527	744 546	760 579	852 775	733 615	757 ***799***	589 606	477 560
744 546	750 560	***852*** 741	754 601	813 794	674 624	650 759	474 562
760 579	***852*** 741	756 592	823 761	703 606	732 ***799***	609 681	462 557
852 775	754 601	823 761	701 586	667 597	659 690	580 717	417 510
733 615	813 794	703 606	667 597	619 600	619 744	483 592	
757 ***799***	674 624	732 ***799***	659 690	619 744	513 620	405 498	
589 606	650 759	609 681	580 717	483 592	405 498		
477 560	474 562	462 557	417 510				

Max. Fuel Tempr. at:

BOC	***852***
EOC	***799***

Figure IV-15: Case 3 - BOC and EOC average fuel temperature map (°C).

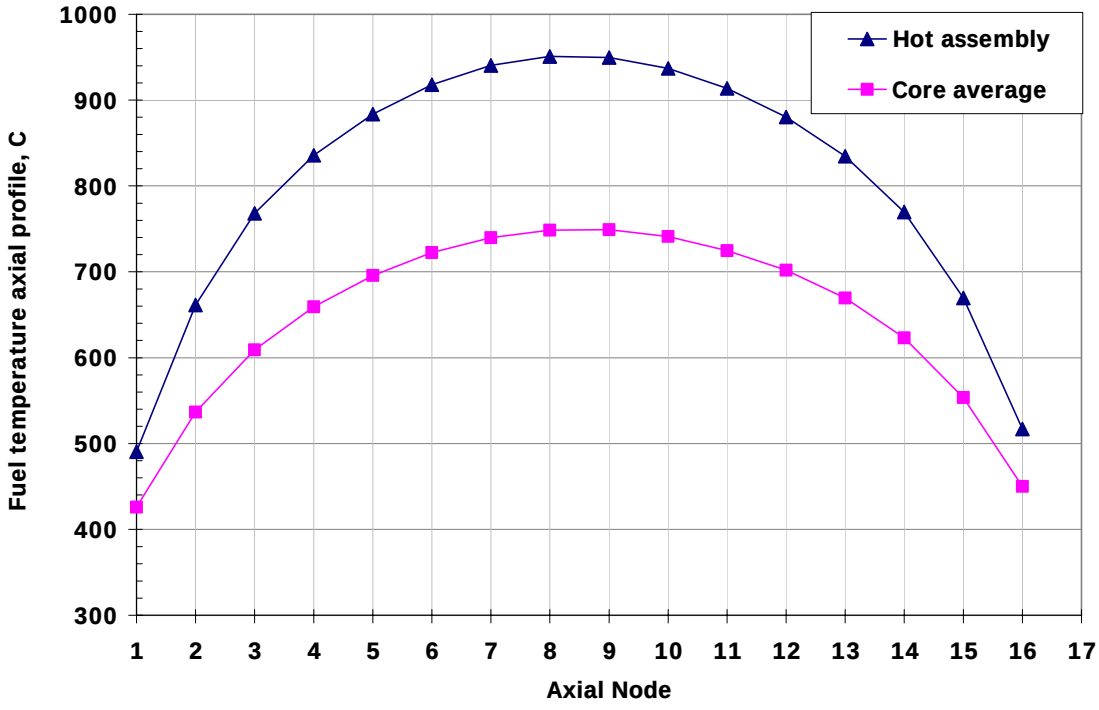

Figure IV-16: Case 1 - BOC axial fuel temperature distribution

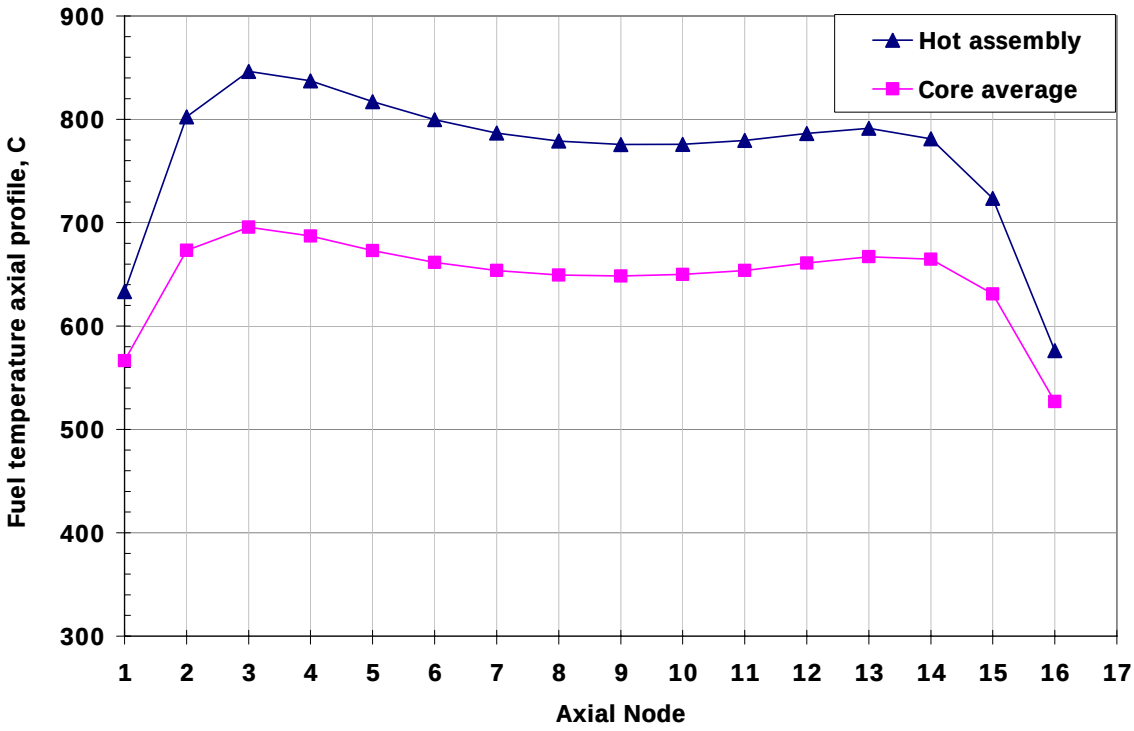

Figure IV-17: Case 1 - EOC axial fuel temperature distribution

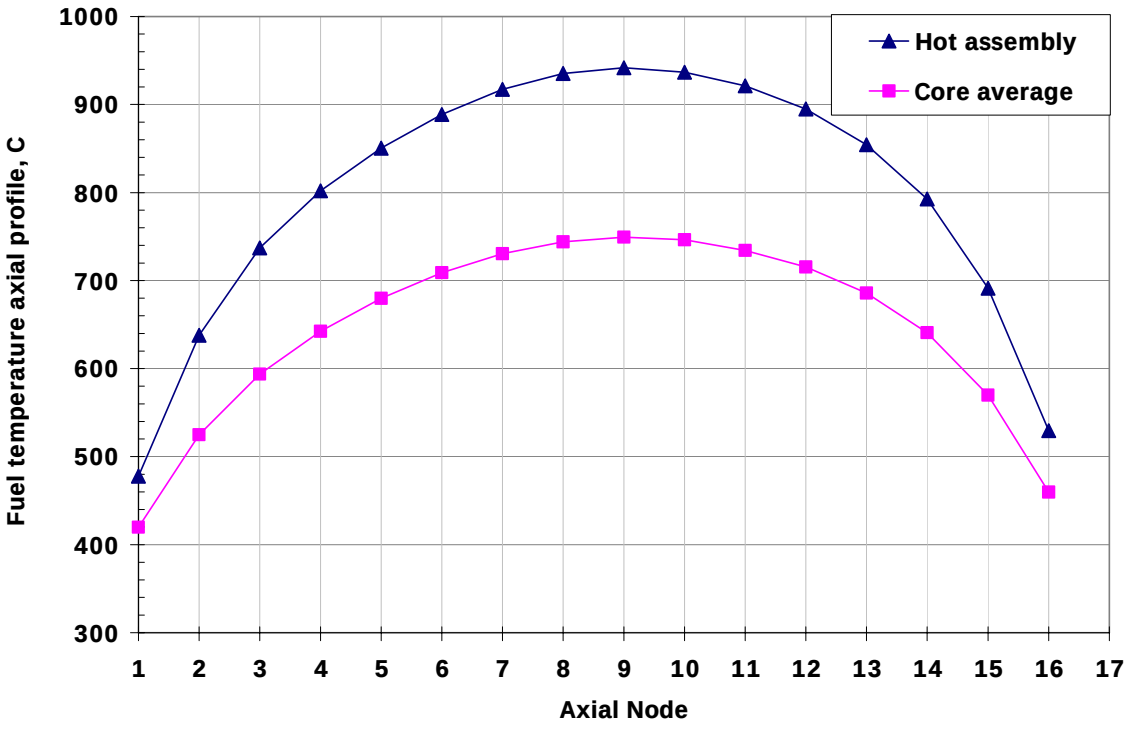

Figure IV-18: Case 2 - BOC axial fuel temperature distribution

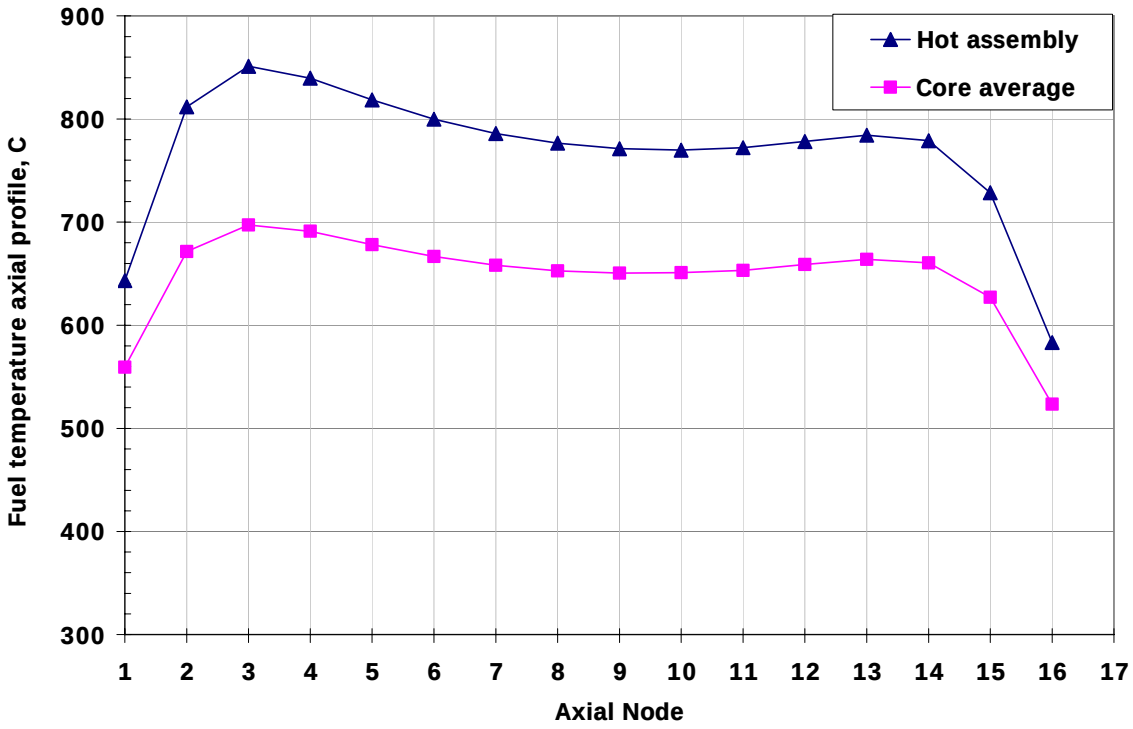

Figure IV-19: Case 2 - EOC axial fuel temperature distribution

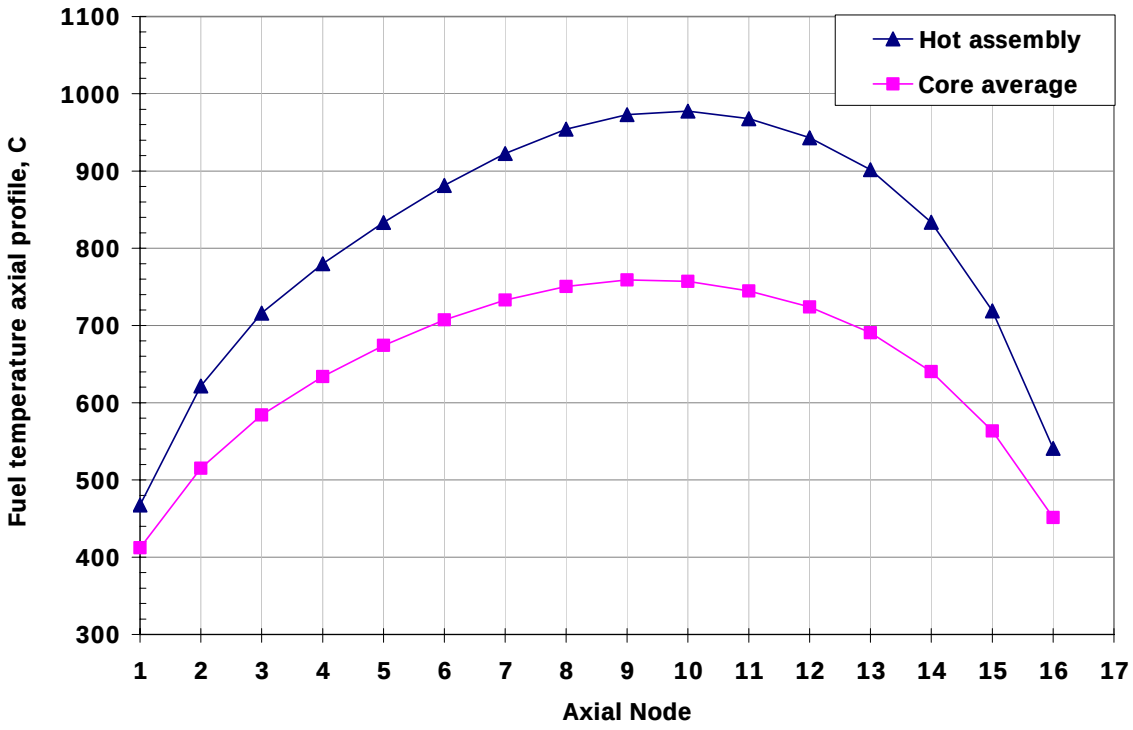

Figure IV-20: Case 3 - BOC axial fuel temperature distribution

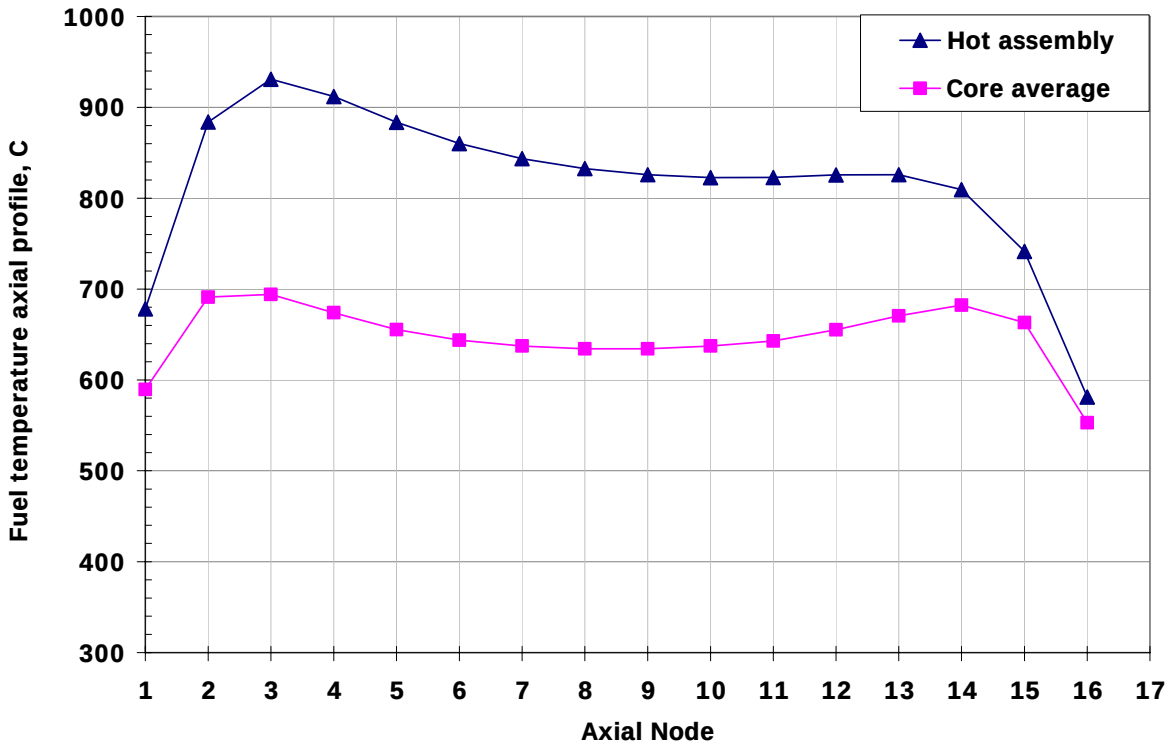

Figure IV-21: Case 3 - EOC axial fuel temperature distribution

IV.4 Summary and Conclusions

In this task, we performed 3-dimensional full core simulation of the most promising fertile free MgO-ZrO_2 matrix fuel designs selected in the previous tasks on the basis of 2-dimensional assembly level analysis.

The objective was to calculate major core performance parameters, reactivity feedback coefficients and fuel temperature distribution for FFF cores and compare these parameters with those of the reference all-UO_2 and all-FFF (PSI design) cores.

The calculations were performed with SILWER computer code, which was modified to allow treatment of non-UO_2 fuels and annular fuel pellets in the fuel temperature calculation module. A standard 3400MW PWR core was used as reference for the calculations.

Three burnable poison design options were considered:

- Hf Homogeneously mixed with fuel – Er IFBA coating – Boron WABA
- Er Homogeneously mixed with fuel – Hf IFBA coating – Boron WABA
- Enriched Er Homogeneously mixed with fuel

The results of the analysis show that the use of all three burnable poison options is potentially feasible. All major core performance parameters for the analyzed cases are very close to those of a standard PWR with conventional UO_2 fuel including possibility of reactivity control, power peaking factors, and cycle length.

Among the three analyzed BP design options for the fertile free $MgO\text{-}ZrO_2$ matrix fuel, the Enriched Er option was shown to be the most effective one with respect to the minimal cycle length penalty and efficiency of Pu destruction. This advantage has to be evaluated carefully against considerable costs associated with Er enrichment. The additional two BP options considered in this study exhibit similar performance.

The MTC of all FFF cores is negative at the full power conditions at all times and very close to that of the UO_2 core.

The Doppler coefficient of the FFF cores is also negative but somewhat lower in magnitude compared to UO_2 core. The significance of such difference can only be assessed in a comprehensive analysis of all relevant reactor transients in which Doppler feedback is of major importance. The Homogeneously mixed Hf – IFBA Er (Case 1) design shows a slight advantage in terms of the more negative Doppler Coefficient over the rest of the FFF core designs.

The soluble boron worth of the FFF cores was calculated to be lower than that of the UO_2 core by about a factor of two, which still allows the core reactivity control with acceptable soluble boron concentrations. The lower control rod worth may represent a potential design problem of inadequate shutdown margin. This problem can be addressed either by using extra control rods in the Full-MOX PWRs or by using control rods with enriched boron.

The steady state fuel temperature distributions in FFF cores are also similar to the reference UO_2 core. In the FFF core, the core average fuel temperature is lower than that of the UO_2 core by about 100°C due to the higher thermal conductivity of the MgO-ZrO_2 matrix. However, the maximum fuel temperatures in the hot assemblies in the FFF and the UO_2 cores are very close because of the slightly higher power peaking in the FFF cores which cancels out the effect of the better thermal conductivity.

In summary, the results of the analysis show that the FFF cores with all three considered burnable poison options are potentially feasible. The conclusion is based on the fact that all calculated FFF core performance characteristics are close to those of the reference PWR core with conventional UO_2 fuel. This study had shown that the FFF core characteristics are adequate for the steady state reactor operation.

Further detailed analysis should be performed to ensure the FFF core safety also under accident conditions. Such analysis should take into account the whole spectrum of thermal, mechanical, and neutronic characteristics of the fertile free fuel and therefore is beyond the scope of this project.

References

1. Paratte J.M., Foskolos K., Grimm P., and Maeder C., “Das PSI Codesystem ELCOS zur stationaren Berechnung von Leichtwasserreaktoren”, Proc. Jahrestagung Kerntechnik, Travemunde, p.59, Germany, May 17-19 (1988).

2. Kasemeyer U., Paratte J.M., Grimm P., Chawla R., "Comparison of Pressurized Water Reactor Core Characteristics for 100% Plutonium-Containing Loadings," Nuclear Technology,122, pp. 52-63, April (1998).

3. Paratte J.M., Grimm P., and Hollard J.M., “User’s Manual for the Library Preparation Code ETOBOX”, PSI, CH-5232 Villingen PSI, (1995).

4. Paratte J.M., Grimm P., and Hollard J.M., “User’s Manual for the Fuel Assembly Code BOXER”, PSI, CH-5232 Villingen PSI, (1995).

5. Paratte J.M., Grimm P., and Hollard J.M., “CORCOD User’s Manual”, PSI, CH-5232 Villingen PSI, (1991).

6. Fridman E., Kolesnikov S., Shwageraus E., Galperin A., “Dissolution, Reactor, and Environmental Behavior of ZrO_2-MgO Inert Fuel Matrix: Neutronic Evaluation of MgO-ZrO_2 Inert Fuels,” Department of Nuclear Engineering, Ben-Gurion University of the Negev, Final Report for University of Nevada, Las-Vegas (June 2005). Available from: http://aaa.nevada.edu/task19.html

7. Galperin A., Grimm P., Raitzes V., “Modeling And Verification of The PWR Burnable Poison Designs by ELCOS Code System”, Annals of Nuclear Energy, 22, Pages 317-325, (1995).

8. Medvedev P., “Development of dual phase magnesia-zirconia ceramics for light water reactor inert matrix fuel”, Ph.D. thesis, Texas A&M University, (2004).

9. Todreas N., Kazimi M., “Nuclear Systems I Thermal Hydraulic Fundamentals”, Taylor&Francis, Levittown, PA, (1993).

10. Fridman E., Galperin A., and Shwageraus E., “Dissolution, Reactor, and Environmental Behavior of ZrO2-MgO Inert Fuel Matrix: Neutronic Evaluation of MgO-ZrO2 Inert Fuels,” Task 3, Year 2 Progress Report, Department of Nuclear Engineering, Ben-Gurion University of the Negev, (2005).

11. Fridman E., Galperin A., and Shwageraus E., “Dissolution, Reactor, and Environmental Behavior of ZrO2-MgO Inert Fuel Matrix: Neutronic Evaluation of MgO-ZrO2 Inert Fuels,” Task 1, Year 2 Progress Report, Department of Nuclear Engineering, Ben-Gurion University of the Negev, (2005).

12. Grossbec M. L., Renier J.-P. A., and Bigelow T., “Development of improved burnable poisons for Commercial nuclear power reactors”, Final Report on NERI Project Number 99-0074, (2003).